EXPERIMENTAL METHODOLOGY TO ASSESS THE EFFECT OF COATINGS ON FIBER PROPERTIES USING NANOINDENTATION

A Thesis
Presented to
The Academic Faculty

by

Juan Pablo Aguilar

In Partial Fulfillment
of the Requirements for the Degree
Master of Science in
Mechanical Engineering

Georgia Institute of Technology
December 2012

EXPERIMENTAL METHODOLOGY TO ASSESS THE EFFECT OF COATINGS ON FIBER PROPERTIES USING NANOINDENTATION

Approved by:

Dr. David W. Stollberg, Advisor
GTRI Electro-Optical Sys Labs
Georgia Institute of Technology

Dr. Antonia Antoniou, Advisor
School of Mechanical Engineering
Georgia Institute of Technology

Dr. Kyriaki Kalaitzidou
School of Mechanical Engineering
Georgia Institute of Technology

Date Approved: August 07, 2012

ACKNOWLEDGEMENTS

This research was sponsored in part by DARPA and the Naval Surface Warfare Center, as well as funding from Dr. Stollberg and Dr. Antoniou. Additional support for this research came from the National GEM Consortium. I would like to thank my advisors Dr. Stollberg and Dr. Antoniou for their guidance, support, and encouragement throughout my graduate career. I am also very grateful for my thesis committee, composed of my advisors and Dr. Kalaitzidou, for their time and effort in helping me with the preparation of my thesis.

I would like to thank the various people in my lab at GTRI and at the MiRC who have helped me throughout my graduate career. Thanks to Dr. Ready for his support, advice, and leadership; Stephan Turano for his help and insight regarding deposition, profilometry, and microscopy; Dr. Nadler for his advice and for allowing me to use his equipment; and Walter Henderson for his insight and help with the Hysitron Triboindenter. I would also like to thank the following current and previous graduate students for their help with various tools: Graham Sanborn, Kavin Manickaraj, Justin Nguyen, Ran Liu, Yuan Li, and Ricardo Aguilar.

Lastly, I would like to extend a special thanks to the people in my life who have made my graduate education possible. Thanks to my girlfriend, Lauren Everett, for her love and encouragement; my parents for their love, guidance, and unconditional support; and my brothers, family, and friends for their encouragement. I would not have been able to accomplish this without their constant love and support.

TABLE OF CONTENTS

LIST OF TABLES

LIST OF FIGURES

SUMMARY

Current body armor technologies need further improvements in their design to help reduce combat injuries of military and law enforcement personnel. Kevlar-based body armor systems have good ballistic resistance up to a certain ballistic threat level due to limitations such as decreased mobility and increased weight [1,2]. Kevlar fibers have been modified in this work using a nano-scale boron carbide coating and a marked increase in the puncture resistance has been experimentally observed. It is hypothesized that this improvement is due to the enhancement of the mechanical properties of the individual Kevlar fibers due to the nano-scale coatings. This study presents a comprehensive experimental investigation of individual Kevlar fibers based on nanoindentation to quantify the cause of the enhanced puncture resistance. The experimental setup was validated using copper wires with a diameter size in the same order of magnitude as Kevlar fibers. Results from nanoindentation did not show significant changes in the modulus or hardness of the Kevlar fibers. Scanning Electron Microscopy revealed that the coated fibers had a marked change in their surface morphology. The main finding of this work is that the boron carbide coating did not affect the properties of the individual fibers due to poor adhesion and non-uniformity. This implies that the observed enhancement in puncture resistance originates from the interaction between fibers due to the increase in roughness. The results are important in identifying further ways to enhance Kevlar puncture resistance by modifying the surface properties of fibers.

CHAPTER 1

INTRODUCTION

1.1 Motivation

The research presented in this thesis explores the use of nanoindentation to study the effect of boron carbide (B_4C) coatings on Kevlar fibers. In a previous study, B_4C coatings were applied to Kevlar fabric yielding an improvement in puncture resistance (Figure 1). It is hypothesized that this improvement is due to the enhancement of the mechanical properties of the fibers due to the nano-scale coatings, and a nanoindentation methodology is proposed to evaluate the effect of these coatings. The aim of this research is employ the use of boron carbide coatings on Kevlar fibers to improve the ballistic and puncture resistance of Kevlar-based body armors. As weapons technology progresses, so does the ballistic threat against soldiers. This continuously increasing threat is both in terms of bullet caliber and available energy [1]. As such, improving body armor has become a major initiative in recent years. In fact, in 1998, improving body armor was listed as one of the Department of Defense's (DoD) "Top Ten Tough Problems," falling under the heading of soldier survivability/mobility/lethality [2].

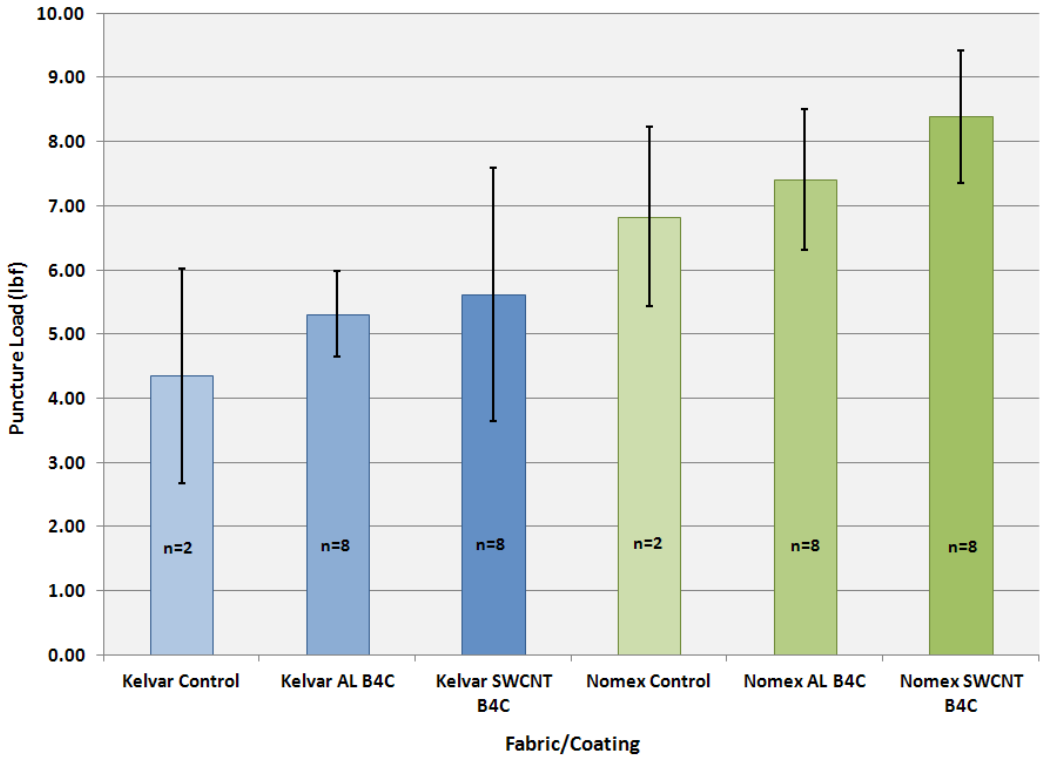

Figure 1. Puncture resistance of fabrics coated with boron carbide

1.2 Body Armor

The main types of personnel armor systems being employed include 'soft', flexible armors and ceramic-based, 'rigid' armor plates [1]. The type of armor required for different situations depends on the threat level as designated by the National Institute of Justice (NIJ) [2]. Table 1 shows the different threat levels and the armor classification system adopted by the NIJ. These body armor standards require that projectiles be stopped upon impact, and that the penetration depth into a clay slab behind the armor does not exceed 1.73 in [3]. Further penetration of a projectile can lead to serious blunt trauma [1, 4].

Soft body armor is capable of defeating threat levels up to Type II-A. For threat levels higher than that, rigid armor systems are employed [2]. Modern flexible armors

are typically comprised of several layers of high-tenacity para-aramid fiber fabrics [1]. Such armor was based on the development of Kevlar by the DuPont Corporation. Body armor made from multiple layers of Kevlar fabric was originally developed by the Army's Edgewood Arsenal and the Natick R&D Command in the 1970s [2].

Table 1. NIJ Body Armor Classification [3]

NIJ Body Armor Class	Ballistic Threat That the Armor Will Defeat
Type I	0.22 LR; most handguns ≤ 32 caliber 0.38 special, lead bullet (<850 ft/s)
Type II-A	0.357 Magnum, soft point (<1250 ft/s) 9 mm pistol, metal jacket (<1090 ft/s) 0.45 auto, and 0.38 special +P
Type II	0.357 Magnum, soft point (<1395 ft/s) 9 mm, metal jacket (<1175 ft/s)
Type III-A	0.44 Magnum, lead bullet (<1400 ft/s) 9 mm submachine gun, metal jacket (<1400 ft/s)
Type III	High powered rifle 7.62 NATO metal jacket (<2750 ft/s) 5.56 NATO metal jacket 12-gauge shotgun rifled slug
Type IV	Armor-piercing rifle 0.30 caliber armor piercing (<2850 ft/s) single hit protection against lesser threats

Current rigid armor plates in use typically consist of three different components: a ceramic strike face that is hard and brittle which acts to erode the bullet and dissipate energy, an energy absorbing backing typically made of aramid fiber fabric, and an epoxy adhesive layer binding the two. Figure 2 illustrates a typical ceramic armor plate made of boron carbide, capable of stopping a 12.7 mm bullet [1]. Figure 3 illustrates the mechanism by which the plate system stops a bullet. When the projectile hits the plate, the ceramic structure fractures and also erodes the surface of the bullet.

Figure 2. Commercial boron carbide armor plate [1]

Deformation in the armor system propagates through the ceramic into the aramid backing in a cone shaped fashion. The backing distributes and absorbs the energy of the eroded bullet and ceramic fragments over a large area via deformation in the form of stretching of the fibers [1].

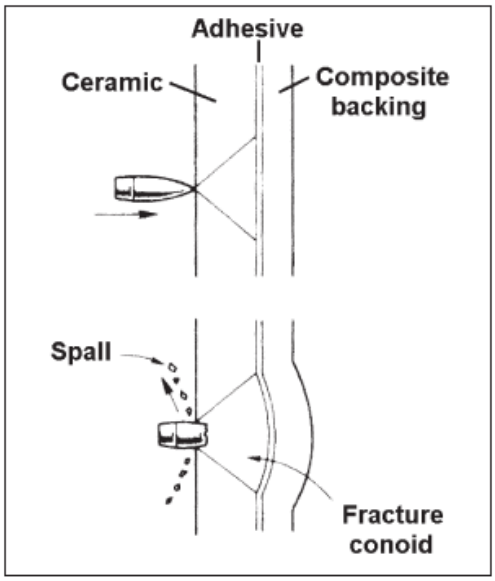

Figure 3. Absorption of ballistic energy by ceramic plate with aramid backing [1]

One of the main issues with this type of armor is that they are heavy and make it difficult for the soldier to operate while wearing them. In fact, even the Type III-A vests are so heavy, bulky, and inflexible that they are not considered suitable for routine wear [2]. For this reason, armor designers are searching for ways to create armor systems that minimize weight and thickness, thereby reducing their burden on military personnel [1].

1.3 Proposed Work

In this thesis, Kevlar fibers are coated with boron carbide, and a new testing methodology is proposed to ascertain the nano-mechanical properties of the individual Kevlar fibers by using nanoindentation. This experimental methodology was first validated by conducting nanoindentation experiments on small diameter copper (Cu) wires. Copper was used because there is a lack of existing research regarding this specific form of testing on Kevlar fibers, and also because the properties of Cu have been well studied and quantified. The results from experimentation on copper wires in this study can compared to tabulated results and used to validate the methodology such that there is a high degree of confidence in the results obtained from testing on Kevlar fibers.

CHAPTER 2

BACKGROUND

2.1 Kevlar Fiber

Soft body armor is based on high-tenacity para-aramid fiber fabrics, such as Kevlar. These high performance fibers are characterized by low density, high strength, and high energy absorption [4]. They consist of highly oriented poly-para-phenylene terephthalamide polymer chains made through a unique shear and slow relaxation process. This process fully aligns the randomly oriented domains in the polymer solution with close to perfect molecular orientation, thereby creating very strong fibers [5]. Standard Kevlar 29 fibers (ballistic grade) have the following properties: filament diameter of 12 μm, breaking strength of 338 N, tensile modulus of 70.5 GPa, specific density of 1.44 g/cm^3, decomposition temperature in air at 427°C, and Poisson's ratio of 0.36 [5].

These properties make Kevlar an exceptional material for lightweight ballistic armor systems. However, to meet the protection requirements for typical ballistic threats, approximately 20–50 layers of fabric are required. The resulting bulk and stiffness of the armor limits its comfort, and has restricted its application primarily to torso protection [4]. Also, it has been found that the properties of the fiber alone do not fully determine the effectiveness of the armor system. Cheeseman and Bogetti [6] identified the following factors as being the primary elements that determine the effectiveness of soft body armor systems: material properties of the fibers, the fabric weave structure, the projectile geometry, the interaction between individual fabric layers, and the inter-yarn and fabric-projectile frictions.

Inter-yarn and fabric-projectile frictions are very important factors that can be modified to improve the ballistic resistance of soft body armor. When these frictions are increased, yarns in an armor made from woven fabric are less likely to slip over one another and over the projectile during ballistic impact; in order to penetrate the fabric, the projectile will have to engage and break more yarns rather than simply pushing them apart. The extra force required to overcome this friction leads to an increased energy absorption capacity of the fabric [7]. Conversely, it has been found that when these frictions are minimized, the performance of the armor decreases. Bazhenov et al. found that wetting Kevlar fabric with water lowered these friction values resulting in both lower pull-out resistance and lower ballistic performance [8].

2.2 Current Improvements on Soft Body Armor Systems

There have been several studies conducted on improving soft body armor systems using different techniques. These techniques include the use of shear thickening fluids [4], [7], hard particles [9], and hard ceramic coatings [10]. These technologies, while effective at increasing the fabric's ballistic resistance, all have major drawbacks including, increased weight and reduction of effectiveness through normal wear and tear due to a loss of liquid or particles from the system. In this study, the fabric was coated with a nano-scale layer of boron carbide, which does not significantly increase the weight, reduce flexibility, or require an external system to hold a liquid or particles within the fabric.

Lee et al. [4] conducted a study in which a shear thickening fluid (STF) composed of 450 nm diameter silica particles dispersed in ethylene glycol is used to impregnate

Kevlar fabric. Shear thickening is a non-Newtonian flow behavior of a fluid, in this case observed in a concentrated colloidal dispersion, that is characterized by a significant and sometimes discontinuous increase in viscosity with increasing shear stress [11]. This phenomenon can be used as a dampening mechanism in which energy from an impact is absorbed [7]. Lee et al. proposed to use this shear thickening property to enhance the ballistic resistance of Kevlar-based, flexible body armor. They carried out a series of tests in which layers of Kevlar fabric were impregnated with different quantities of STF and were then subjected to ballistic tests. Test targets were composed of impregnated samples placed inside Ziplock bags sealed using a heat sealer. This was done to prevent leakage of STF out of the target assembly and to protect the Kevlar fabric from moisture [4], which has been shown to decrease their ballistic resistance [8]. Ballistic resistance was measured in terms of projectile penetration depth and dissipated energy.

Results showed that the addition of STF to the fabric increases the amount of projectile energy absorbed by the target. The STF also significantly increased the weight of the fabric. Despite of the weight increase, the improvement in ballistic resistance was significant enough to make this a viable method to modify Kevlar-based soft body armors. In fact, Lee et al. found that four layers of Kevlar impregnated with 2 mL of STF weigh about the same as ten layers of neat (unimpregnated) Kevlar and are able to dissipate the same amount of energy. Since this is accomplished with four layers rather than ten, the impregnated target is thinner and more flexible than the neat target. The investigators suggested that a possible mechanism by which the addition of STF increases ballistic resistance is by constraining the Kevlar yarns as they are pulled through the

fabric. Figure 4 illustrates the difference in fiber pullout between the neat fabric versus the STF impregnated fabric.

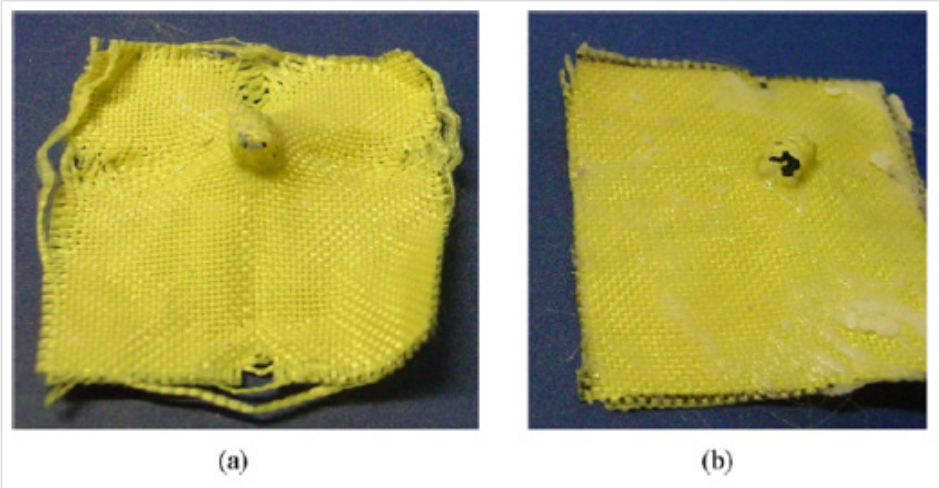

Figure 4. Kevlar fabric after ballistic test: (a) neat, (b) impregnated [4]

Lee et al. suggest that the increase in energy dissipation in the impregnated sample is due in part to the increase in force required to pull the fibers out from the fabric, yielding less pull-out required to absorb the energy from the projectile. They also suggested that this increase in pull-out resistance increases the load excreted on the fibers during impact, enabling them to absorb more energy through fiber deformation and fracture [4].

In 2005, Tan et al. [7] conducted a similar study in which plies of CT615 Twaron fabric (a para-aramid fiber fabric similar to Kevlar) were impregnated with a silica colloidal water suspension (SWS) and ballistic tests were performed to determine the optimum concentration of silica particles in the suspension. The particles used in this experiment had an average diameter of 100 nm. Systems of single, double, and quadruple plies were tested with 0 (neat), 20, 40, and 50 wt% SWS particle concentrations. The ballistic resistant performance of the fabrics was measured in terms

of ballistic limit and specific ballistic energy. The ballistic is the lowest velocity at which the projectile penetrates the armor [7].

Results from the study showed that the SWS improved the performance of all systems. The researchers found that the silica suspension affects the quadruple system to a lesser extent than the double ply system, and that the single ply systems were affected to an ever lesser degree, as illustrated in Figure 5.

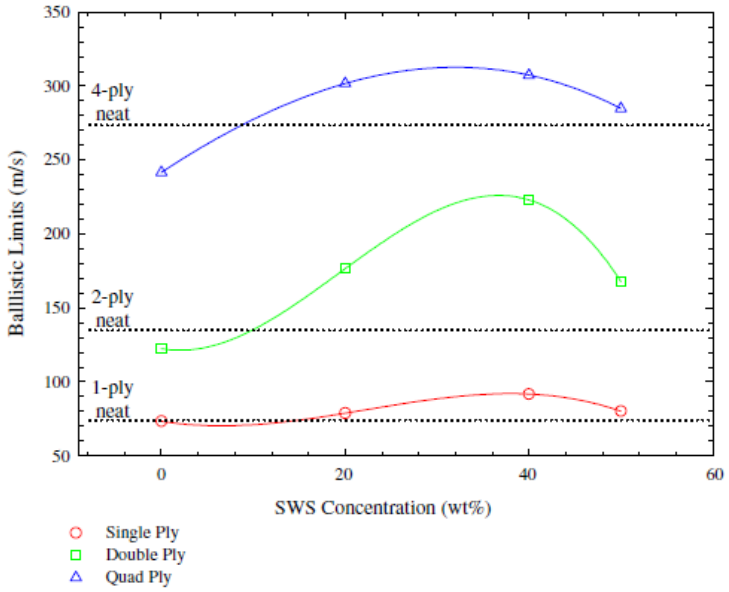

Figure 5. Ballistic limits of single, double, and quadruple ply systems [7]

This suggests that the silica suspension has an effect on the interaction between plies. Systems with one ply are not as sensitive to the SWS, while systems with more than four plies may be too stiff to experience relative ply sliding and therefore do not benefit as much from the SWS.

To get a better representation of the improvement of the armor system through the addition of SWS, specific ballistic energy was calculated. Specific ballistic energy is the energy of the projectile at the ballistic limit divided by the area density of the fabric system. This measure takes into account the added weight from the impregnation of the

fabric with the colloidal suspension. It was found that the greatest improvements occurred in the double ply system with 40 wt% SWS, with a specific ballistic energy of 0.414 J/g/m^2 (compared to about 0.210 J/g/m^2 for the double ply neat system) [7].

These studies showed that in general, adding STF limits the mobility of yarns within a fabric, thereby increasing the resistance of the fabric to damage modes typical of ballistic impact such as yarn pull-out [4, 9]. However, they offered very limited insight on the mechanisms by which the STF and fabric interact to produce these beneficial properties. In a study by Kalman et al., these mechanisms were explored further. Specifically, the effect of particle hardness is explored by comparing fabric treatments containing particles of different hardness: SiO_2 particles, which are significantly harder than Kevlar, and poly(methyl methacrylate) (PMMA) particles which are softer [9]. The silica particles used were 500 nm in diameter and had a density of 1.96 g/cm^3; the PMMA particles used were bigger, with a diameter of about 1050 nm and a density of 1.23 g/cm^3. Poly(ethylene glycol) (PEG) was used as the carrier fluid for both the SiO_2 and the PMMA STF's [9].

The experiments consisted of ballistic tests on neat fabrics, STF-coated fabrics, and dried STF-coated fabrics (leaving the particles behind). Results from the study show that overall, the addition of particles into fabrics, dry or wetted, leads to an increase in fabric resistance to ballistic penetration. The particles in the fiber do not alter the mechanical properties of the fiber itself, and therefore, the improvement in resistance is due to changes in the mobility-driven defeat mechanisms such as yarn sliding and pull-out. Results also showed that the hardness of the particles is an important factor in the behavior of particle-intercalated fabrics. The experiments demonstrated that fabrics with

harder particles (SiO_2) have higher resistance than those with softer particles (PMMA). The investigators suggested two possible explanations for this phenomenon. One explanation is that harder particles are able to be embedded into the softer polymer filaments, resulting in a greater degree of mechanical coupling between the fibers and particles. Another possible explanation is that the softer particles are more likely to deform under stress. Such accommodation could lead to less resistance to bulk compression and reorganization mechanisms, resulting in a lower degree of influence in fiber mobility within the fabric [9].

Kalman et al. found that the addition of STF to the fabrics as opposed to purely dry particles increased friction between fibers and increased fiber pull-out resistance. The addition of STF treatments also showed a slight decrease in the ballistic resistance of the fabrics compared to the dry particle treatment. These results suggest that just simply reducing yarn mobility is not always beneficial; there exists an optimal degree of mobility for a given fabric and threat combination [9].

On a more practical note, the results of this study also showed that while dry particle systems might have slightly better ballistic resistance, they are not as practical as the wet systems (STF). This is because the fabrics with dry particles tend to shed particles easily as a result of coming in contact with most surfaces or just by being handled roughly. This is to be expected since there is no significant binding force keeping the particles in contact with the fabric beyond van der Waals or other small forces. In contrast, STF systems can be handled roughly without losing the particles. This behavior suggests that the liquid carrier holds the particles in the fabric through a capillary or wetting mechanism [9]. One major drawback from STF systems is that care

must be taken to keep the fabric wet. The fabrics must not be allowed to dry or lose liquid. For this reason, in the experiments by Lee et al. [4], the STF impregnated fabrics had to be placed in sealed Ziploc bags. Any puncture to such assembly could lead to the STF leaking out of the system, thereby decreasing its effectiveness.

Another approach to improving soft body armor, explored by Gadow et al. [10], incorporates the advantages of reducing fiber mobility as well as the advantages of incorporating hard surface materials such as ceramics and cermets (as is the case for rigid armor systems). In their study, they coated high tenacity para-aramid fiber fabrics (Twaron CT 710) with high hardness refractory cermet and oxide ceramics via thermal spraying without damaging the fibers and maintaining fabric flexibility. The goal of the study was to improve the resistance against bullets and blades of soft body armor systems [10].

The fabrics were coated using the Atmospheric Plasma Spray (APS) process, illustrated in Figure 6, which is a thermal spray process that allows the application of a variety of metallurgical, cermetic and ceramic coatings while keeping the thermal load on the substrate relatively low by the use of air or liquid CO_2 cooling techniques.

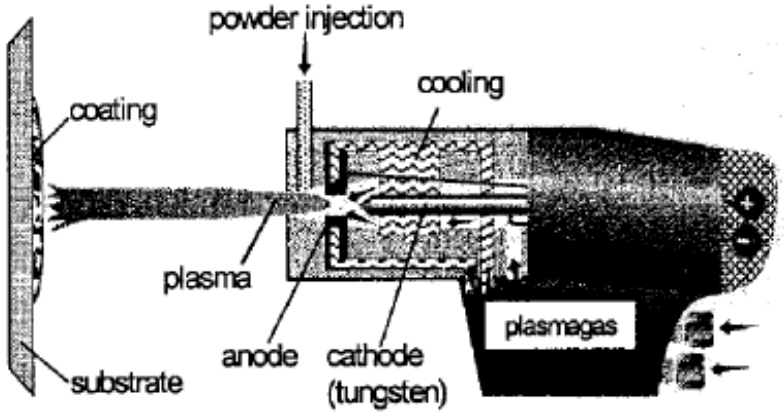

Figure 6. Schematic of an Atmospheric Plasma Spray [10]

This method was used to coat fabrics with Al_2O_3 and TiO_2 ceramics as well as WC Co 83/17 cermet. An AlSi 12 coat was used as a bond coat to improve the adhesion of the coatings to the fabric. The coatings had a thickness of about 75 ± 5 μm and a small degree of microcracks and porosity, which is desirable to maintain fabric flexibility. Care was taken to make sure the porosity was not too high, since this could decrease the hardness and other valuable mechanical properties of the coatings.

Stab resistance tests were carried out to evaluate the performance of the coated fabrics. Results showed an increase in stab resistance for the coated fabrics. The WC Co 83/17 cermet and the Al_2O_3/AlSi 12 mulitylayer coatings showed the best performance in terms of microhardness and bond strength. The penetration work for fabrics with these coatings increased by a factor of five compared to the uncoated fabric. This increase is due to the coating increasing the fiber-to-fiber friction which prevents distortion, making it more difficult for penetrating objects to change the fabric structure and push the fibers aside. The hardness of the coatings also helps by blunting the penetrating objects, increasing the surface area and making it more difficult to penetrate the fabric. This mechanism is illustrated in Figure 7, which shows the amount of blunting experienced by the penetrating blade after six punctures of a single layer of WC Co 83/17 coated fabric. As seen in the figure, the blunting of the blade is significant [10].

Stab resistance tests were carried out to evaluate the performance of the coated fabrics. Results showed an increase in stab resistance for the coated fabrics. The WC Co 83/17 cermet and the Al_2O_3/AlSi 12 mulitylayer coatings showed the best performance in terms of microhardness and bond strength.

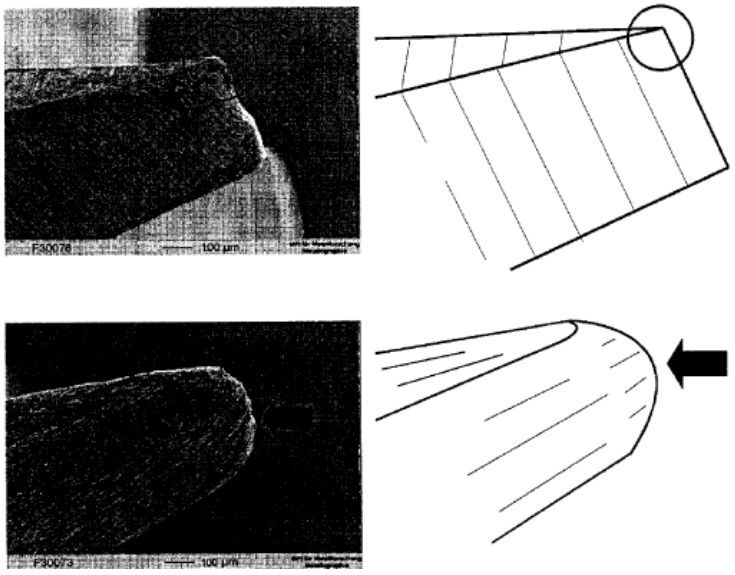

Figure 7. SEM images of blade (top) before and (bottom) after six punctures [10]

The penetration work for fabrics with these coatings increased by a factor of five compared to the uncoated fabric. This increase is due to the coating increasing the fiber-to-fiber friction which prevents distortion, making it more difficult for penetrating objects to change the fabric structure and push the fibers aside. The hardness of the coatings also helps by blunting the penetrating objects, increasing the surface area and making it more difficult to penetrate the fabric. This mechanism is illustrated in Figure 7, which shows the amount of blunting experienced by the penetrating blade after six punctures of a single layer of WC Co 83/17 coated fabric. As seen in the figure, the blunting of the blade is significant [10].

Despite the improvements obtained from the coatings, one of the drawbacks of this technique is the increase in weight. As shown in Figure 8, the addition of the WC Co 83/17 cermet increased the weight of the fabric from 220 g/m^2 to 450 g/m^2, a factor of increase of about 2.05. Similarly, the fabrics with the Al_2O_3/AlSi 12 multilayer coating underwent a weight increased by a factor of about 2.18, from 220 g/m^2 to 480 g/m^2 [10].

This means that an armor vest created using this technique would be about twice as heavy as a regular, unmodified armor.

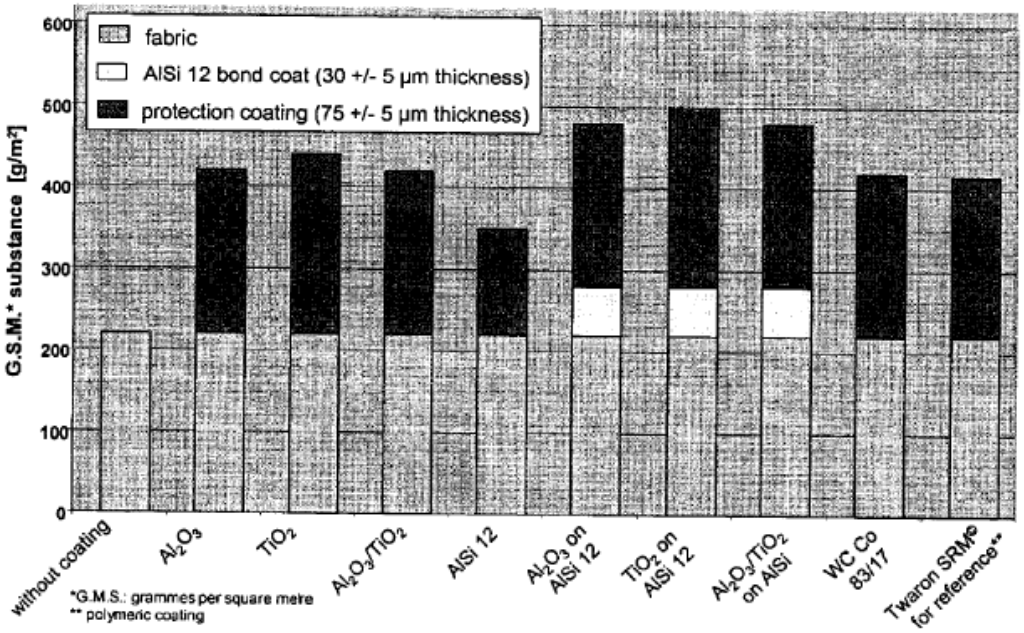

Figure 8. Weight gain of fabrics with protective coatings [10]

2.3 Boron Carbide

In the current study, the ballistic resistance of soft body armors is improved by the addition of a boron carbide (B_4C) thin film. The aim is to create an armor system that will improve on the traditional Kevlar system by dissipating energy through mechanisms similar to those described in previous studies: increasing the fiber-to-fiber friction which reduces mobility, making it more difficult for penetrating objects to change the fabric structure and push the fibers aside [4, 7, 10, 11]; and adding a hard substance which couples the fibers, further helping to reduce mobility and transfer the ballistic energy to more fibers [9] as well as helping to blunt the penetrating objects, increasing their surface area and making it more difficult to penetrate the fabric [10]. An added benefit resulting

from the use of B_4C thin films, as opposed to STFs or spray coated cermet/ceramic coatings, is that the weight added to the fabric from the coating is minimal and the flexibility of the fabric remains unaffected. This allows for an armor system that has improved ballistic resistance without increased burden for the user.

It is hypothesized that a thin coating of boron carbide is able to achieve these goals due to the ceramic's exceptional mechanical properties. It is the third hardest material at room temperature, surpassed only by diamond and cubic boron nitride. In contrast to diamond and cubic boron nitride gradually whose hardness de-creases as temperature rises, boron carbide is characterized by its high thermal stability [12]. B_4C also has low specific weight, high modulus, high chemical stability, and good wear resistance [13]. These properties make it an excellent material to use for ballistic resistance; hence, it is often used for rigid body armor plates. In this study, the outstanding properties of B_4C will be utilized in conjunction with Kevlar fiber without losing flexibility or adding too much weight.

The hardness of boron carbide coatings differ depending on the preparation and the deposition method. In general, the hardness ranges between 29 to 35 GPa [14]. Two common methods for making boron carbide coatings are using chemical vapor deposition (CVD) and plasma assisted chemical vapor deposition (PACVD). These methods use hazardous gasses such as diborane (B_2H_6) boron trichloride (BCl_3) and require very high temperatures. The requirement for high temperatures limits the substrates on to which a coating can be deposited [15]. Substrates such as Kevlar or other para-aramid fibers are unable to be coated with these methods since they degrade at temperatures higher than 400°C [5]. Due to this high temperature deposition requirement with the CVD methods,

research has been done to find other ways to deposit B_4C. Deposition methods such as pulsed-laser deposition [16], ion beam sputtering [13], magnetron sputtering [15, 17], and RF sputtering [18] have been investigated and have been used to successfully create B_4C coatings at lower temperatures.

2.4 RF Sputtering of Boron Carbide

In this study, boron carbide thin film coatings were deposited onto copper wires and Kevlar fibers via RF sputtering. While the most common method to sputter B_4C is using either RF or DC magnetron sputtering, there has also been some research on sputtering B_4C using non-magnetron RF sputtering [18]. In a study by Tavsanoglu et al., 500-700 nm B_4C coatings were deposited onto mirror polished AISI 430 steel and polished Si (100) wafer substrates. Table 2 lists the deposition parameters used for each deposition.

Table 2. Deposition parameters of B_4C coatings [18]

	BC1	BC2	BC3
Base pressure (Pa)	1.33×10^{-6}	1.33×10^{-6}	1.33×10^{-6}
Working pressure (Pa)	0.67	0.26	0.4
Temperature (°C)	250	250	250
Target power (W)	80	140	100
Cathode voltage (V)	500	700	600
Deposition time (h)	8	6	8

The coatings were deposited by RF sputtering (13.56 MHz) using a commercial boron carbide target of 99.5% purity. High-purity Argon gas (99.999% pure) was utilized as the plasma gas. No external heating was used during the deposition; however, due to the long deposition times, the temperature increased until it reached a steady-state at 250°C, as indicated in Table 2. The working pressure, target power, and cathode voltage were the main parameters that were varied to evaluate their influence on the

properties of the deposited film. The hardness and Young's modulus of the deposited coatings were analyzed by nanoindentation using a Hysitron Triboscope [18].

Results from the study show coating thicknesses of 700 nm, 520 nm, and 720 nm for samples BC1, BC2, and BC3 respectively, with the low thickness of BC2 resulting from the lower deposition time. Overall, the average rate of deposition was about 1.5 nm/min. The reason for this is the non-magnetron design as well as the low sputtering yields of the boron and carbon under argon bombardment.

A series of nanoindentation measurements were carried out to characterize the coatings. Results from the nanomechanical testing are shown in Figure 9. The coatings showed about 70% elastic recovery after unloading, indicating that boron carbide coatings have high elasticity. It is apparent from Figure 9 that modifying the selected deposition parameters has little influence on the hardness and Young's modulus of the coatings. The coatings were found to have a hardness of about 22 GPa and a Young's modulus of about 240 GPa [18].

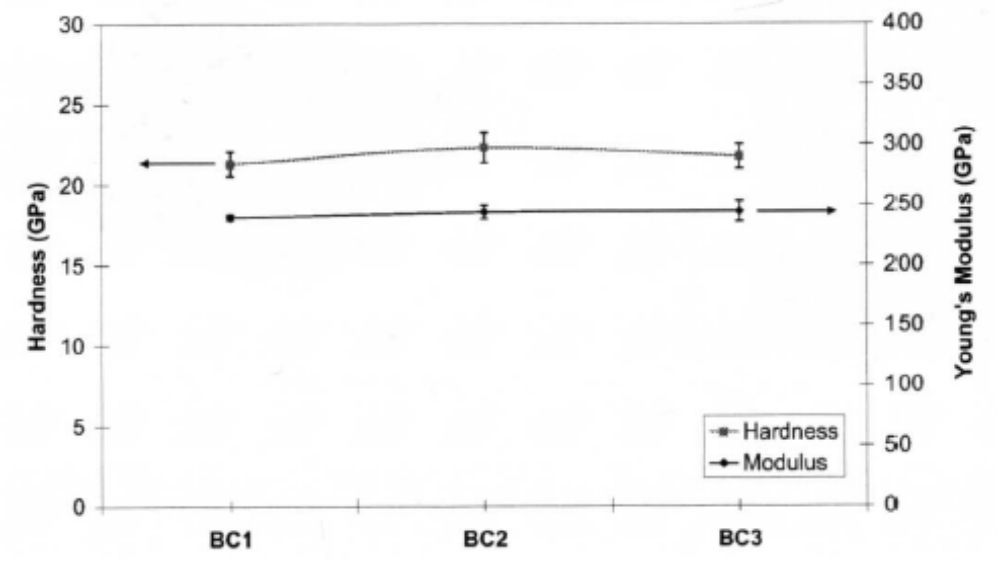

Figure 9. Hardness and Young's Modulus of B_4C coatings [18]

2.5 Nanoindentation

In order to understand the ballistic resistance mechanisms of yarn and fabric materials in soft body armor systems, it is important to understand the mechanical properties of single fibers [19]. In this study, it is hypothesized boron carbide coatings will enhance the mechanical properties of individual fibers and as a result improve the properties of the overall Kevlar fabric. For this reason, it is important to be able to probe the properties of the individual fibers and to be able ascertain the effects of the coating on these properties. To achieve this, nanoindentation was chosen as the primary means of evaluating the properties of the Kevlar fibers and the corresponding boron carbide coatings. The hardness and Young's modulus of the fibers with and without the coatings were evaluated via nanoindentation using a Hysitron Tryboindenter.

Nanoindentation is a technique that can be used to assess mechanical properties of materials at a very small (submicron) scale. This technique is similar to bulk hardness testing techniques in which an indenter of a specific shape is driven into the surface of a material and its response is measured. The difference in nanoindentation is that the loads applied are in the millinewton range and the indentation depths are on the micro to nanometer range. Such small force and indentation depth allows for the deformation of very small volumes of material, making it an ideal tool for the investigation of mechanical properties of small samples, specific regions of samples such as individual grains, and very thin films/coatings. This technique can be used to derive values for mechanical properties of materials such as hardness, elastic modulus, and toughness.

The indenter tip used for nanoindentation plays a big role in the determination of material properties. Parameters such as size, shape, and material properties must be taken

into account. Indenter tips are very small and can be of various shapes including Berkovich (three sided pyramid), cube corner, Vickers (square based pyramid), conical, and flat cylinder, among others. The tip is usually made out of diamond, or other hard materials such as sapphire, quartz, tungsten carbide, and others depending on the application. In this study, a Berkovich, single crystal diamond tip was selected with a tip radius of approximately 150 nm [20].

The main properties being studied in this research are hardness and elastic modulus. These properties cannot be measured directly from a nanoindentation test, but rather, are derived from the measured response. A nanoindentation event yields data regarding the applied force used during the indent and the displacement of the material being indented, and it typically takes the form of a load-displacement graph, as shown in Figure 10 [21]. This data is then used to obtain a hardness value and an elastic modulus value for the test material.

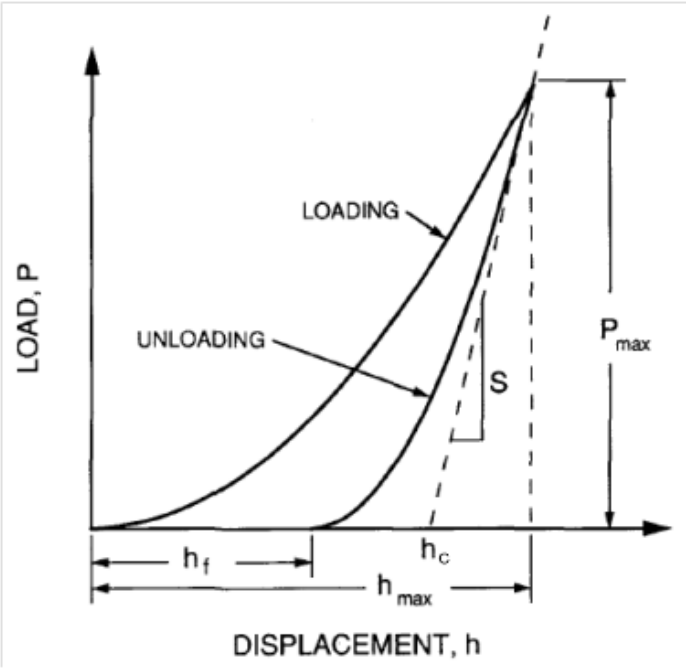

Figure 10. Typical load vs. displacement curve for a nanoindentation test [21].

Figure 10 illustrates the response of the material as the tip indents the material. The loading curve shows the displacement into the test material made as the force on the indenter is increased. As the force is removed (the unloading phase), there is some elastic recovery of the material. The quantity P_{max} denotes the maximum force used during the experiment and it corresponds with the maximum displacement measured on the material, labeled as h_{max}. The displacement h_f is the final displacement depth of the material after the load has been completely removed. Other important parameters shown on the graph are h_c, known as the contact depth, and the initial unloading stiffness, *S* [21]. The contact depth is the vertical depth on which contact is made with the indenter.

Doerner and Nix experimented with nanoindentation to determine hardness and modulus. They developed a method to derive these values using the measured load and displacement data. This approach, however, assumes linear unloading [22], which has been found to be an inaccurate assumption. As a result, a new method of analyzing load-displacement data was proposed by Oliver and Pharr [21]. The parameters used in the analysis are illustrated in Figure 11.

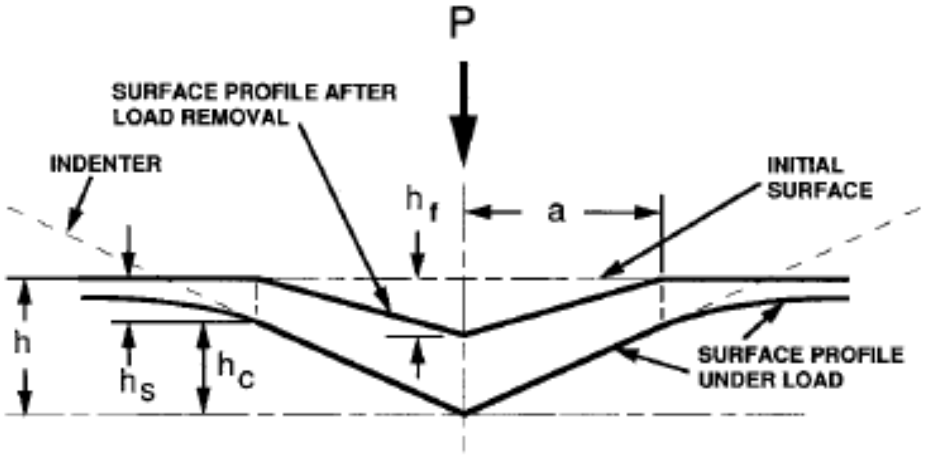

Figure 11: Schematic of a section through an indentation [23]

The total displacement of the indentation (h_{max}) is written as follows [21]:

$$h_{max} = h_c + h_s \tag{1}$$

where, the terms h_s the displacement of the surface at the contact perimeter. The penetration depth at peak load (h_{max}) can be measured directly, and displacement of the surface at the contact perimeter (h_s) can be ascertained from the indenter geometry according to the following equation [21], where ϵ is the geometric constant that correspond to the indenter shape.

$$h_s = \epsilon \frac{P_{max}}{S} \tag{2}$$

The contact stiffness S is estimated from the indentation data by taking into account the top 10% of the unloading curve and calculating the slope, as shown on Figure 10. Once the contact area is established, it can be used to calculate the hardness via the following equation:

$$H = \frac{P_{max}}{A} \tag{3}$$

Upon further examination, it was found that the unloading behavior of a many materials can be described by a single indenter geometry. The best geometry to describe the data was found to be the paraboloid geometry, with a value for ϵ of 0.75 [21]. This is due to the fact that when plasticity occurs, the pressure distribution that forms around the tip of the indenter is more similar to that predicted by the paraboloid geometry. The area function for a Berkovich indenter was estimated as follows:

$$A(h_c) = 24.5h_c^2 + C_1h_c^1 + C_2h_c^{1/2} + C_3h_c^{1/4} + ... + C_8h_c^{1/128} \tag{4}$$

where C_1 through C_8 are constants, found by an iterative method using the first term as a start [21]. The elastic modulus of the material can then be calculated using the following equation,

$$\frac{1}{E_r} = \frac{1-\nu^2}{E} + \frac{1-\nu_i^2}{E_i} \tag{5}$$

where E_r is the reduced modulus, E and ν are the Young's modulus and Poisson's ratio of the test specimen, and E_i and ν_i are the corresponding values for the indenter [24] (1140 GPa and 0.07 respectively) [20]. The reduced modulus of the system takes into account the deformation of both the test specimen and the indenter tip, and can be calculated using the estimated stiffness value with Equation 6 [25]:

$$E_r = \frac{\sqrt{\pi}}{2\beta}\frac{S}{\sqrt{A}} \tag{6}$$

where β is a constant that depends on the indenter geometry (β = 1.034 for a Berkovich tip [26]).

This method offers a way to estimate the hardness and elastic modulus of test specimen given the measured load and displacement curves from a nanoindentation event; however, this method does not guarantee that these quantities are completely accurate. A small degree of error is assumed. The value for stiffness, which is used in the calculation of both the elastic modulus and hardness of the material, is estimated by using part of the unloading curve. However, using more or less of the data from the unloading curve will yield different values for stiffness. Similarly, the area function is different for each individual indenter and is estimated by using statistical analysis on empirical data. Since these two quantities are not directly measured but rather are derived from measured quantities, a small amount of error is introduced into the

calculation of other properties based on these derived quantities, i.e. hardness and elastic modulus.

2.6 Nano-mechanical Properties of Copper

In this study, nanoindentation was used to assess the properties of the surface of Kevlar fibers and the boron carbide coatings applied to them. In previous studies, Kevlar fibers have been embedded in epoxy and polished prior to testing [27, 28]. Such a procedure does not allow for the investigation of the surface of the fiber or any coating that is applied to it. For this reason, a new methodology was proposed which involves mounting Kevlar fibers horizontally on silicon wafers using adhesive and conducting nanoindentation tests their surface perpendicular to the fiber axial direction. Due to a lack of previous research on Kevlar using this specific methodology, nanoindentation experiments were first conducted on copper wires. The aim of experimenting on copper wires was to validate this methodology such that the results from nanoindentation on Kevlar could be considered to be accurate representations of the fibers' properties.

Copper was chosen because its bulk properties are known and have been tabulated. However, like other polycrystalline materials, its mechanical properties are affected by the specimen's grain size [29]. In a 2006 study, Chang and Chang explored the properties of copper films using nanoindentation [30]. They conducted nanoindentation tests on pure copper samples of with different grain sizes to determine the grain size effect on the nano-mechanical properties of the copper samples. An optical microscope, a scanning electron microscope, and a transmission electron microscope were used to determine the average grain size of the different specimen. Chang and

Chang tested high purity copper samples with grains sizes ranging between 10 nm to 40 μm.

The copper samples tested included bulk copper in the form of rolled copper plates, sputtered copper films with a thickness of 2 μm, electroplated films with a thickness of 2-3 μm, and electrolessly deposited copper films with a thickness of 1-2 μm. The different samples went through varying annealing processes resulting in a wide range of grain sizes. The hardness and modulus of the samples were found via nanoindentation using a UMIS nanoindenter with a Berkovich tip (~ 100 nm tip radius). Table 3 lists all the different samples tested along with their corresponding grain sizes and the reported nano-mechanical properties.

Table 3. Grain sizes and mechanical properties of Cu samples [30]

	Bulk Cu				Sputtered Cu			Electroplated Cu			
Specimen annealing (°C)	700	600	500	400	300	200	100	400	300	200	None
Grain size (nm)	40 100	20 500	14 300	12 300	501	266	140	4530	1560	560	43
STDV	5030	2640	2950	1520	55	56	18	532	352	73	19
Hardness (GPa)	1.04	1.07	1.07	1.11	1.63	1.71	1.89	1.29	1.41	1.61	2.26
STDV	0.06	0.09	0.08	0.08	0.36	0.23	0.21	0.11	0.11	0.13	0.25
Modulus (GPa)	124	128	125	128	127	117	121	134	134	131	131
STDV	25.1	49.0	26.2	29.2	22.8	23.9	33.1	27.3	30.0	31.7	35.3
Shear stress (GPa)	1.36	1.33	1.33	1.33	1.32	1.31	1.33	1.34	1.33	1.39	1.39
STDV	0.10	0.10	0.04	0.08	0.06	0.11	0.12	0.08	0.08	0.10	0.10

CHAPTER 3

EXPERIMENTAL PROCEDURE

3.1 Overview

Puncture tests on boron carbide coated Kevlar fabric indicated an increase in the puncture resistance of the fabric after the coating was applied. It is hypothesized that the effect of this coating on the mechanical properties of individual fibers is the reason for the improvement in the overall fabric performance. A new methodology for exploring the mechanical properties of plain and coated Kevlar fiber via nanoindentation is proposed. Nanoindentation was chosen over other common mechanical test methods such as Dynamic Mechanical Analysis (DMA) because nanoindentation is able to probe the localized effects of the coating whereas DMA measures overall bulk properties. Prior to performing nanoindentation on Kevlar fibers, this methodology was first validated by conducting nanoindentation tests on copper wires. This was done by comparing the results from nanoindentation tests on copper to tabulated values [30]. The method derived for nanoindentation on wires and fibers is a follows: the wires/fibers were adhered to silicon substrates with an adhesive that was spun-coated on to the substrates. These samples were then coated with boron carbide by way of RF sputtering. Nanoindentation was conducted on coated and uncoated samples. A schematic of the sample preparation and nanoindentation procedure can be found in Appendix A. Table 4 contains the physical properties of the specimen tested.

Table 4. Physical properties of samples tested

Material	Diameter (μm)	Average Grain Size
Copper Wire	50.0	3.8±0.37 μm
Kevlar Fiber	12.0	Polymer

3.2 Spin Coating Adhesive

The wires and fibers were mounted the silicon substrates using ethyl cyanoacrylate adhesive (super glue). In order to prevent the adhesive from covering the wire and thereby altering the results from nanoindentation, only a very thin layer of adhesive was applied to the substrate. This was done by way of spin coating, which allows for the adhesive to be deposited as a very thin conformal layer in a consistent, reproducible manner. Henkel Duro Super Glue was the adhesive used to bond the wires and fibers to the silicon substrates. The adhesive was first diluted with acetone to decrease its viscosity. A 5:1 adhesive to acetone ratio by weight was used. This was also done to decrease the curing speed of the adhesive, allowing sufficient time to place the test specimen on the adhesive before it cures. A Laurell Technologies Corporation, model WS-400-6NPP spin coater was used to deposit the adhesive coatings.

A spin speed vs. thickness of adhesive coating curve was created in order to identify at what spin speeds the adhesive mixture must be deposited to achieve the desired thickness (Figure 13). This was done by first spin coating five 2" round glass substrates with adhesive at different spin speeds – 1500, 2500, 3500, 4500, and 5500 rpm for 30 seconds. On each glass substrate, four ¼" by ½" pieces of Kapton tape were placed in a cross pattern along the edges, as illustrated in Figure 12, prior to the deposition of the adhesive. This tape was used to aid in the determination of the film thickness.

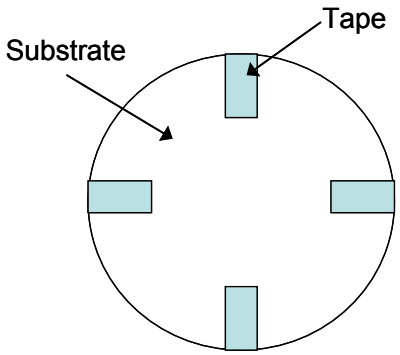

Figure 12. Pattern of tape on glass substrate

The glass substrates were allowed to dry for 24 hours after the adhesive was deposited. The tape pieces were then removed and contact profilometry was performed using a Dektak 150 Profilometer to measure the thickness of the deposited films. The thickness of the films was then plotted with respect to spin speed. Figure 13 shows the relationship between spin speed and thickness of the spin coated adhesive mixture.

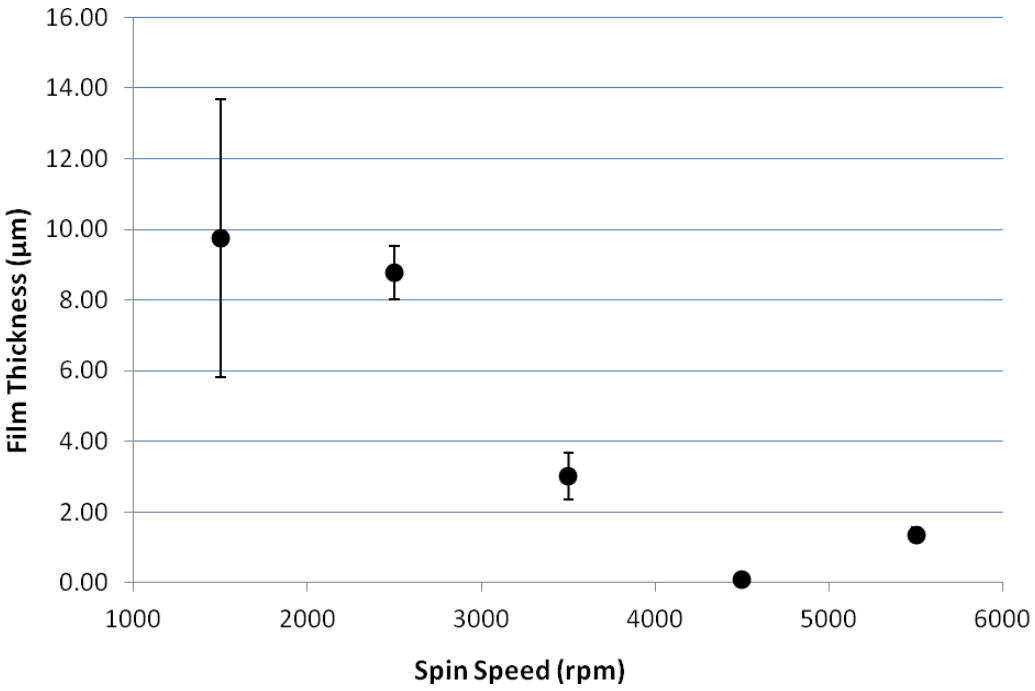

Figure 13. Average spin speed vs. film thickness of spin coated adhesive

3.3 Adhesion of Test Specimen onto the Substrate

The plot in Figure 13 was used to determine the speed at which each substrate must be spun in the spin coater in order to obtain the desired thickness of adhesive. To bond the test specimen to the substrates, adhesive coatings were used with a thickness between 15-25% of the diameter of the test specimen. For the copper wires (50 μm in diameter), a 9 μm thick adhesive coating was used, and for the Kevlar fibers (12 μm in diameter), a 3 μm thick adhesive coating was used. Such thickness ensured that the specimen were well adhered to the substrate without being covered by the adhesive.

After applying the correct thickness of adhesive onto the substrates, the test specimen (copper wires or Kevlar fibers) were placed on the substrate. Care was taken to ensure that specimen did not get covered by the adhesive and that there was full contact between the specimen and the substrate. This was done by first securing the wires/fibers between two pieces of tape, as illustrated in Figure 14, and then carefully setting the assembly on the adhesive coated silicon substrate, ensuring that the wires/fibers make full contact with the substrate.

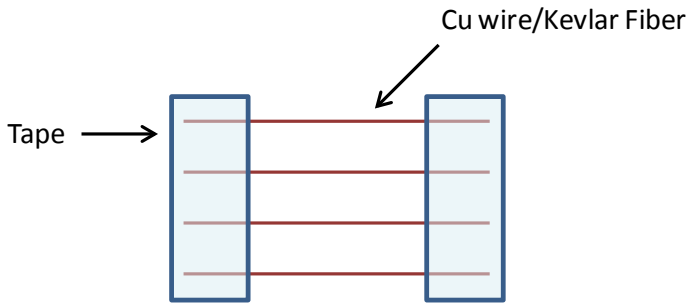

Figure 14. Copper wires or Kevlar fibers secured between two pieces of tape

Once the wires/fibers were placed on the silicon substrates, they were allowed to dry for a period of 24 hours to ensure a full cure. The silicon was then cut into small pieces about 1 cm^2 using a diamond tip scribe such that each piece contained a section of wire or fiber.

Care was taken to ensure that the wires or fibers did not delaminate during the procedure. These small samples were then bonded to 15 mm steel AFM specimen discs using super glue.

3.4 Copper Wire Nanoindentation

As demonstrated by Chang and Chang [30], the hardness and modulus of copper is affected by the grain size of the sample. Therefore, prior to the nanoindentation testing the grain size of the wires was determined. The copper wire used in this study is of 99.9% purity, is 50 μm in diameter, and was obtained from ESPI Metals. Sections of the wire were cast in epoxy and were then polished to achieve a smooth, flat surface. The wires were then submerged in a 5.5 v% Ferric Chloride ($FeCl_3$) solution for 10 seconds [31]. This chemical wet etch process was used to reveal the grain boundaries in the wires (Figure 15). The samples were then immediately rinsed with de-ionized water to prevent further etching. The grains were imaged in an optical microscope to estimate the grain sizes in each wire. The average grain size of the 50 μm wires was found to be 3.8±0.37 μm.

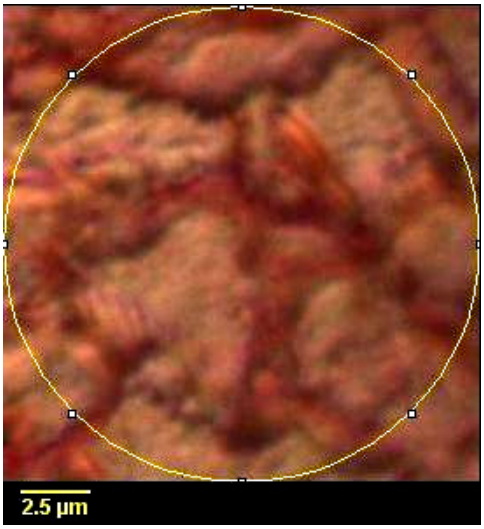

Figure 15. Grains in etched copper wire

Sections of Cu wire were cut and adhered to silicon substrates. Nanoindentation was carried out using a Hysitron Triboindenter equipped with a diamond Berkovich tip with a tip radius of 150 nm [20]. Prior to indenting on the wires, the indenter was first calibrated. The indenter was calibrated in z-direction by conducting an air-indent procedure. Next, the indenter was calibrated in the x-y plane by conducting a series of indentations on an aluminum sample in an "H-pattern". Lastly, a final calibration was conducted by way of a series of indentations on a quartz sample to calculate an appropriate area function for the indenter tip being used. This area function was then used to estimate the Young's modulus and hardness of the subsequent nanoindentation tests on Cu wire and Kevlar fibers.

Tests on the wires consisted of a series of 20-25 indents using the load control mode on the indenter. Some tests were done over a wide range of indentation depths with a peak load starting from 100 μN and systematically increased to a final peak load of 2000 μN over the span of 25 indents. Other tests were carried out over a smaller span of indentation depths with a peak load starting from 25 μN and systematically increased to a final peak load of 1000 μN over the span of 20 indents. The indents were carried out along the central axis of each wire and were separated by a distance of 40 μm for the first set of indents and by 30 μm for the second set of indents, as illustrated in Figure 16. The modulus and hardness values of the wire were then calculated according to the area function.

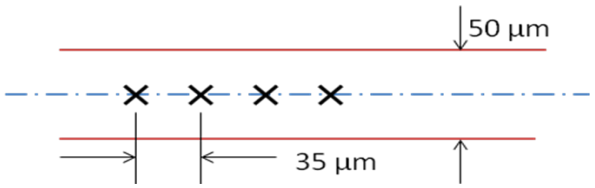

Figure 16. Arrangement of indents on Cu wire on 2nd set of indentation tests

3.5 Nanoindentation of B_4C Coated Samples

Kevlar fibers were adhered to silicon substrates using the same procedure used to adhere the copper wires. Nanoindentation tests were then conducted on the fibers. The indentation procedure started with a peak load of 25 μN and was increased to 1000 μN over the span of 20 indentations. The separation distance between indentations was 30 μm.

The Kevlar fiber and copper wire samples were then coated with boron carbide. This was done via RF sputtering using an Angstrom Engineering EvoVac Deposition System. The deposition was carried out with 200 Watt RF power and 10 mTorr pressure. The plasma gas used was argon, and the gas flow rate was 10 sccm. The film was deposited at a rate of approximately 0.05Å/s over a period of 2 hours, resulting in a film thickness of approximately 36 nm. Prior to coating the samples with boron carbide, the samples were first coated with a 3 nm thick layer of aluminum, also via RF sputtering. This aluminum layer acts as an adhesion layer between the B_4C and the wires and fibers.

After modifying the samples with boron carbide, nanoindentation was performed. The copper wires were indented with a starting peak load of 50 μN, which systematically increased to 2000 μN over a span of 25 indents. The separation distance between indents on the copper wires was 30 μm. The coated Kevlar fibers were indented with a starting peak load of 25 μN, increased to 1000 μN over a span of 25 indents. The separation distance between indents on coated Kevlar fibers was 25 μm. Results from nanoindentation on the coated samples was then analyzed and compared to the nanoindentation results on the uncoated samples.

CHAPTER 4

RESULTS AND DISCUSSION

4.1 Puncture Testing on B_4C Coated Fabric

Prior to conducting this nanoindentation study, the investigator conducted a similar study in 2010 at the GRTI nanolab in which sections of the same Kevlar fabric as well as Nomex fabric were coated with boron carbide. The fabrics were coated with a thin layer of aluminum (10 nm) as an adhesion layer, followed by a 30 nm boron carbide layer, both deposited via RF sputtering. Some samples were impregnated with single wall carbon nanotubes (SWCNT) instead of using an aluminum layer, and then coated with boron carbide. These modified fabrics were tested to determine the effect of the coating on the puncture resistance of the fabric. Figure 1 illustrates the results from puncture resistance testing on the fabrics following ASTM F1342: Standard Test Method for Protective Clothing Material Resistance to Puncture.

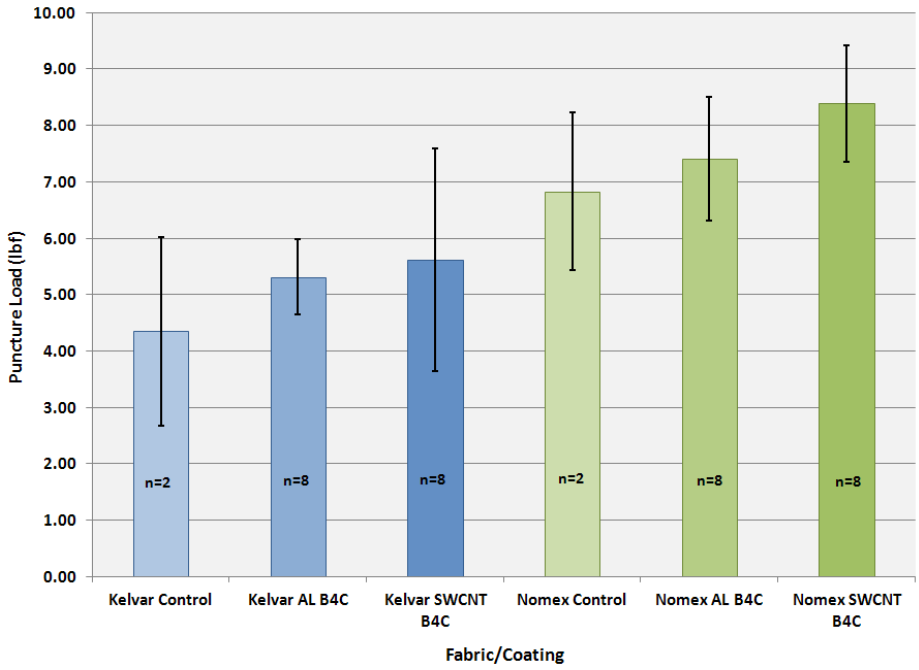

Figure 1. Puncture resistance of fabrics coated with boron carbide

Results from puncture testing are not completely conclusive due to the small sample sizes and large amount of variance. In spite of this variance, results demonstrate an increase in puncture resistance for the coated fabrics: an increase of 1 lbf for Kevlar and 0.7 lbf for Nomex.

4.2 Nanoindentation on Copper Wires

In the current study, several nanoindentation tests were conducted on sections of 50 µm copper wire. The samples were prepared according to the method described in the experimental procedure. Results from the nanoindentation tests on these samples are presented in Figures 17 and 18. Figure 17 is a graph of the average reduced modulus of the wires with respect to indentation depth.

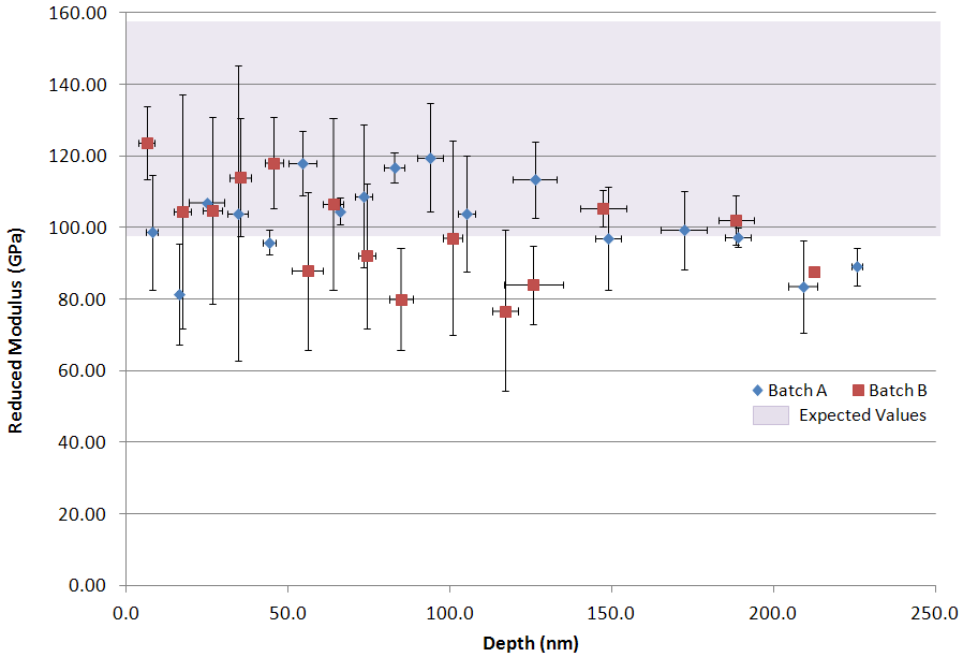

Figure 17. Average reduced modulus vs. indentation depth of copper wires

As described by Equation 5, the reduced modulus is a function of the Young's modulus and Poisson's ratio of the test specimen and the indenter [24]. In the current study, since the modulus of the diamond indenter tip is so high (1140 GPa) [20], the difference

between the reduced modulus and the actual material modulus is negligible. Although there is some variance in the data, the modulus of the wires tends to fall between 90-130 GPa, which is commensurate with tabulated results [30]. Figure 18 is a graph of the average hardness values of for each batch of samples with respect to indentation depth.

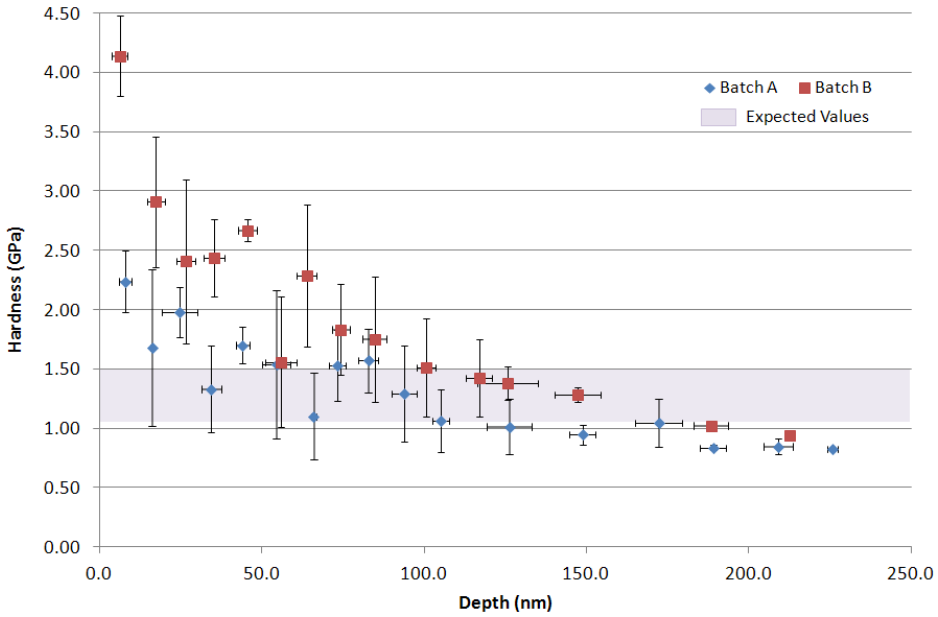

Figure 18. Average hardness vs. indentation depth of copper wires

The hardness values at lower contact depths (0-50 nm) are greater than at higher contact depths. This is due to the presence of an oxide layer on the copper wires. Beyond a contact depth of 50 nm, the average hardness of the wires falls between 1-2 GPa, which is commensurate with the tabulated data [30]. These results suggest that nanoindentation along with the method used to prepare the samples can be used to ascertain the properties of the surface of wires and fibers.

4.3 Nanoindentation of Plain and Coated Kevlar Fibers

After conducting tests on the copper wires, nanoindentation was carried out on Kevlar fibers. The fibers were tested with and without the boron carbide coating. Results from nanoindentation on the fibers are illustrated in Figures 19 and 20. The blue

diamonds in the figures represent the reduced modulus and hardness of the unmodified Kevlar samples and the red triangles represent the modulus and hardness of the Kevlar samples coated with boron carbide.

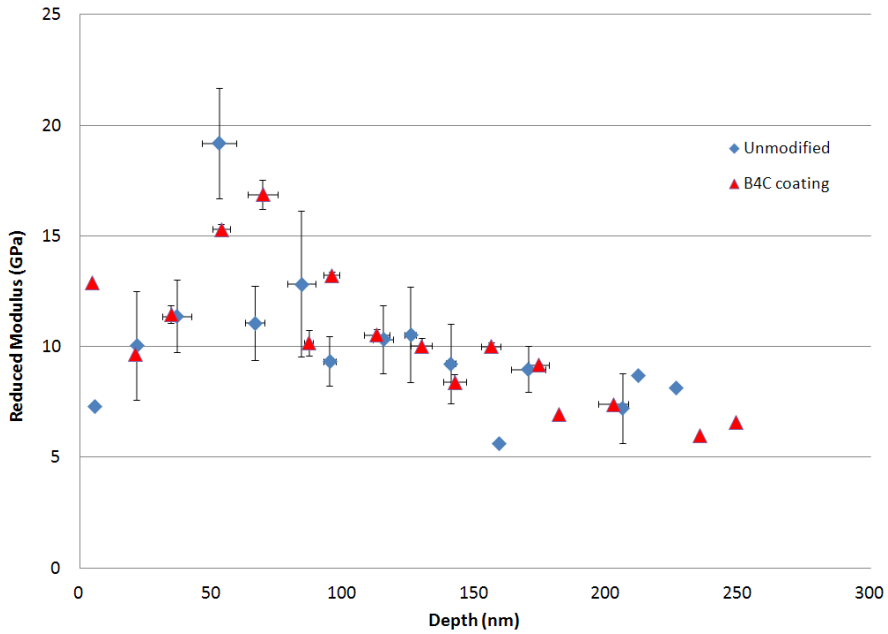

Figure 19. Reduced modulus of unmodified and modified Kevlar fiber

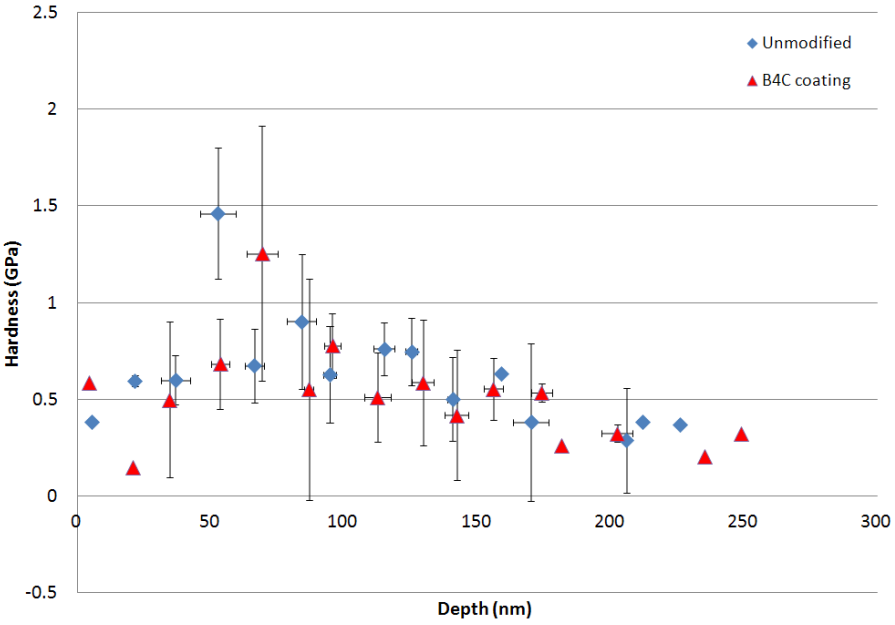

Figure 20. Hardness of unmodified and modified Kevlar fiber

Nanoindentation results indicate values for the reduced modulus and hardness of modified samples that are comparable with those of unmodified samples. Such results suggest that the coating did not have a significant effect on these properties. Further investigation on the nature of the coating was carried out to explore possible reasons for such results.

Scanning electron microscopy (SEM) and optical microscopy were used to image Kevlar fibers with and without the boron carbide coating. Figure 21 is an optical image and Figure 22 is a scanning electron image of an unmodified Kevlar fiber. As seen from these images, the surface of the fiber is relatively smooth with very few anomalies. SEM images reveal a few ridges along the axial direction of the fiber, but an overall smooth surface.

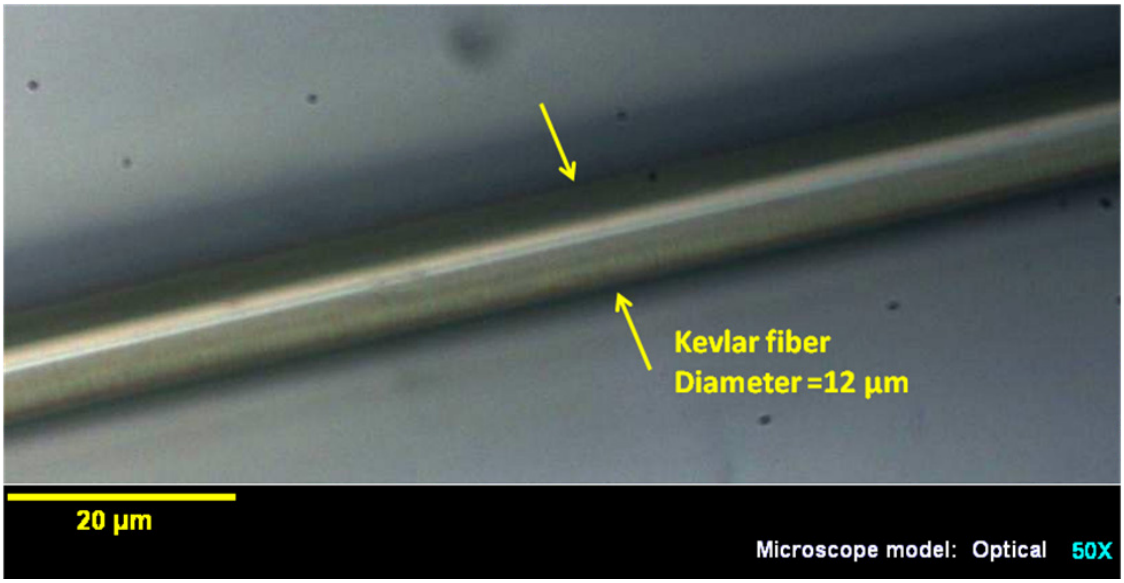

Figure 21. Optical image of unmodified Kevlar fiber (50X)

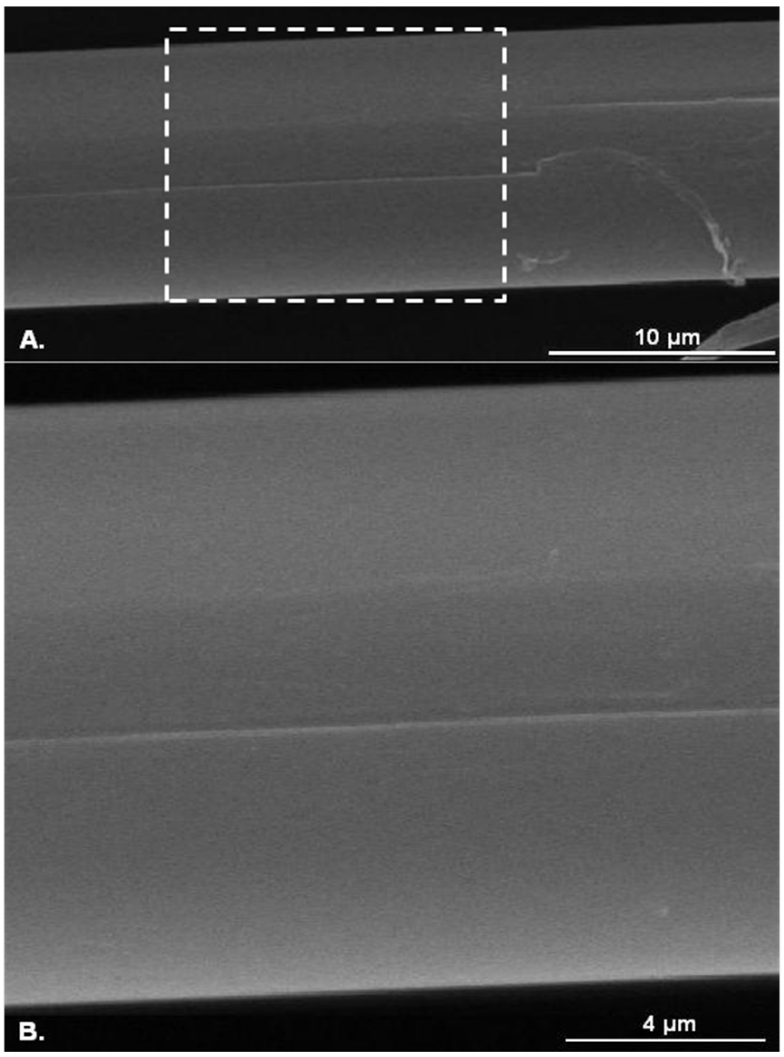

Figure 22. SEM image of unmodified Kevlar fiber: A. Fiber, B. Close-up of fiber surface

Figure 23 is an optical image and Figure 24 is a scanning electron (SEM) image of a Kevlar fiber coated with 3 nm of Aluminum and 30 nm of Boron Carbide. The optical image shows some texture on the surface of the fiber. The coating does not appear to be conformal. Further analysis of the SEM images reveals a coating on the fiber. The coating is rough and non-uniform. The images suggest the coating did not adhere perfectly, and there were signs of delamination.

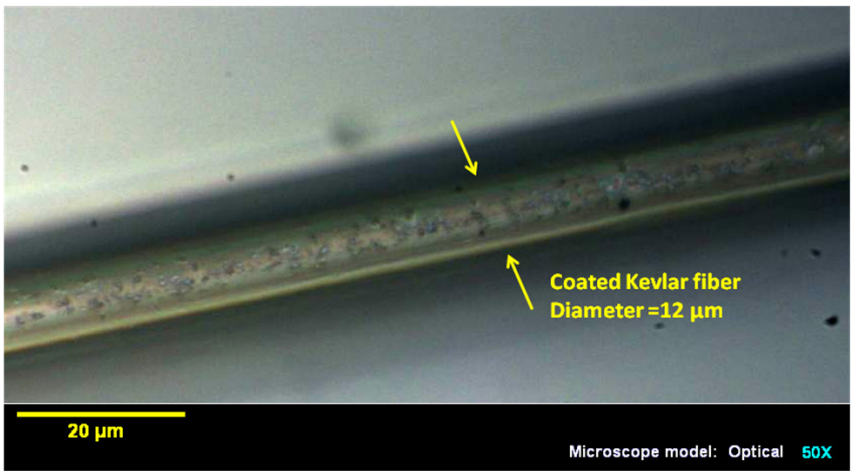

Figure 23. Optical image of Kevlar fiber coated with B_4C

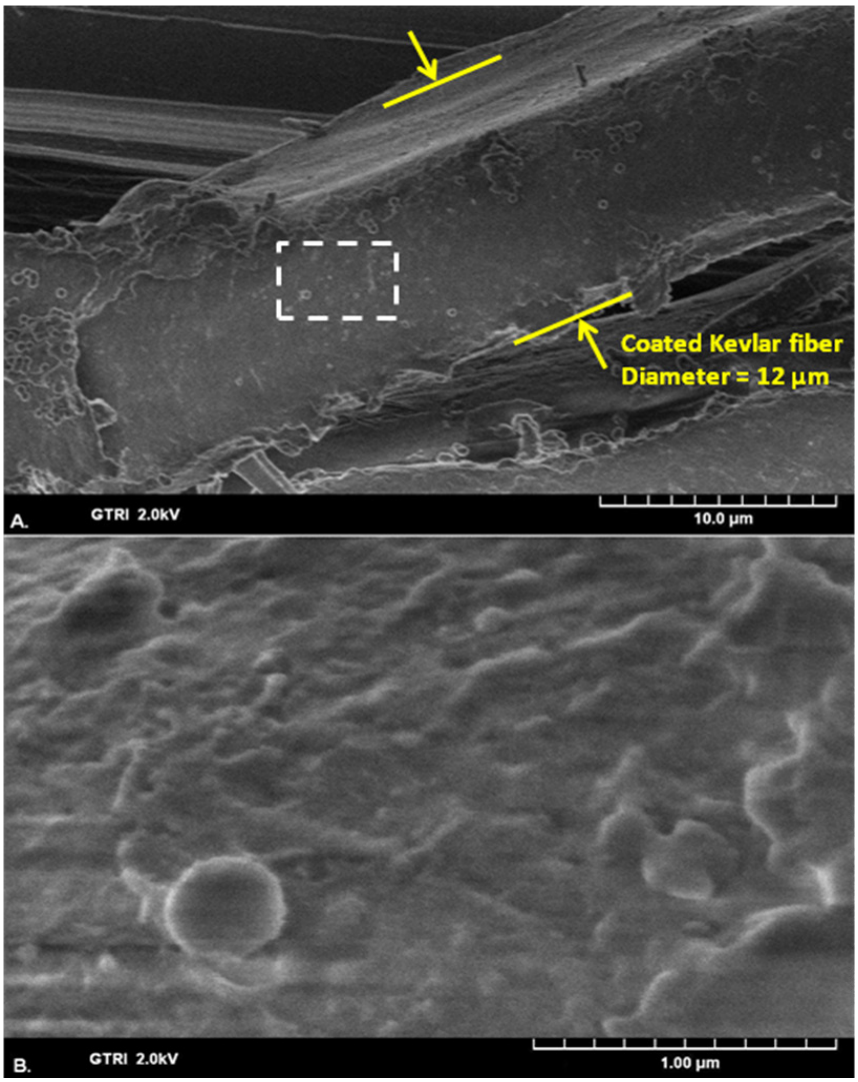

Figure 24. SEM image of coated Kevlar fiber: A. Coated fiber, B. Close-up of coating

In order to confirm that the coating on the fiber was boron carbide, energy-dispersive X-ray spectroscopy (EDS) was used on a Zeiss Ultra60 SEM with an INCA X-ray microanalysis system and a Silicon detector. Table 5 shows the results from EDS.

Table 5. Elemental composition of coated Kevlar fiber

Element	App Conc.	Intensity Corrn.	Weight%	Weight% Sigma	Atomic%
B	11.75	0.6907	14.42	1.12	17.02
C	98.88	1.5245	55.00	1.02	58.44
N	4.12	0.4801	7.27	0.91	6.63
O	44.15	1.7634	21.23	0.59	16.93
Al	2.71	1.0979	2.09	0.18	0.99
Totals			100.00		

Elemental analysis from EDS revealed a significant presence of boron, about 14 weight percent, which resulted from the boron carbide coating. EDS was also able to detect a small amount of aluminum, about 2 weight percent, which comes from the adhesion layer. Figure 25 illustrates the EDS spectrum for the coated Kevlar fiber.

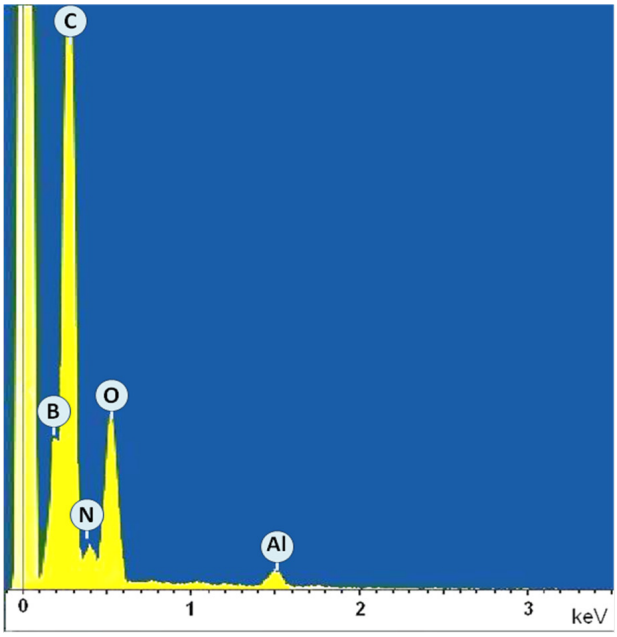

Figure 25. EDS spectrum of coated Kevlar fiber

4.4 Nanoindentation of Coated Copper Wire

The modulus and hardness of the Kevlar fiber was not significantly affected by the boron carbide coating. This might be due to the poor adhesion of the coating. While EDS confirmed the presence of boron carbide and aluminum, SEM and optical microscopy show that the quality of the coating is poor. SEM microscopy also revealed places where the coating seemed to delaminate or did not adhere to the fiber at all. Similar results were obtained from coating the copper wire with aluminum and boron carbide. Figures 26 and 27 are graphs of the average reduced modulus and hardness of the copper wires after the coating. As evident in these graphs, the coating on the copper did not have a significant effect on the modulus or hardness of the copper wires.

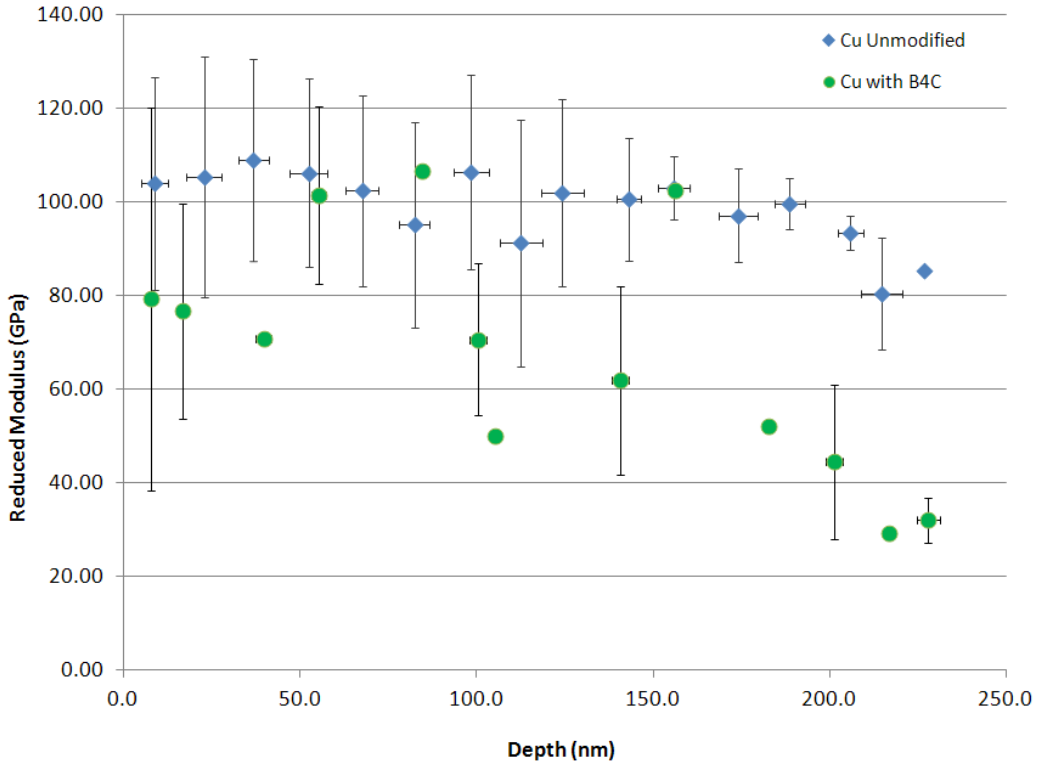

Figure 26. Average reduced modulus of copper wire with B_4C coating

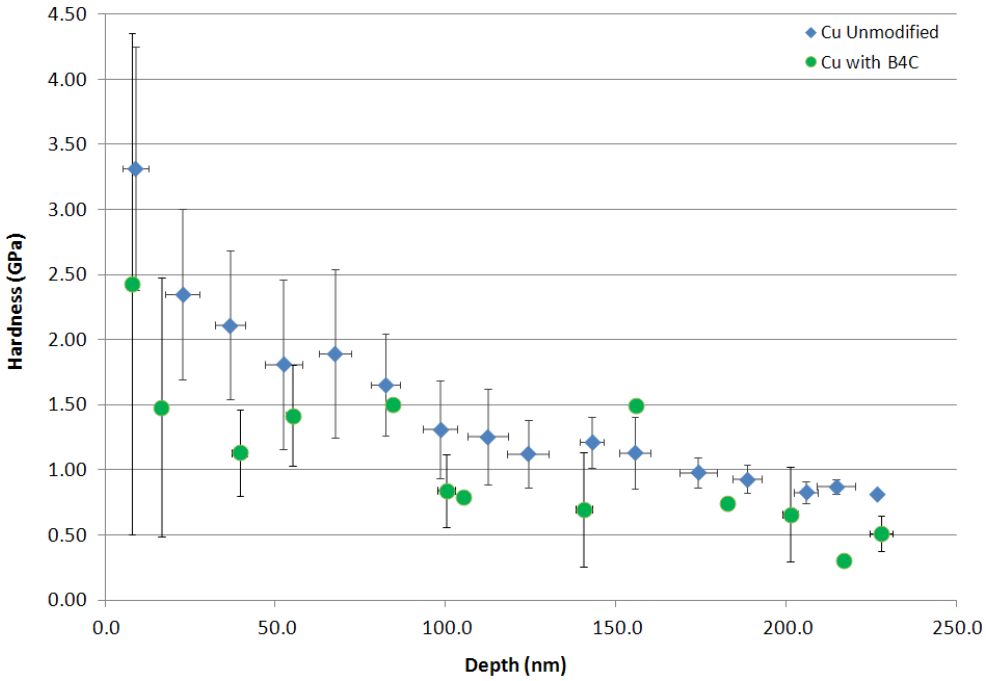

Figure 27. Average hardness of copper wire with B_4C coating

Figures 28 and 29 are optical and SEM images of the unmodified copper wire. As seen in these images, the surface of the copper wire has ridges along the surface that resulted from the drawing process used to produce them. Apart from these ridges, their surface is relatively smooth.

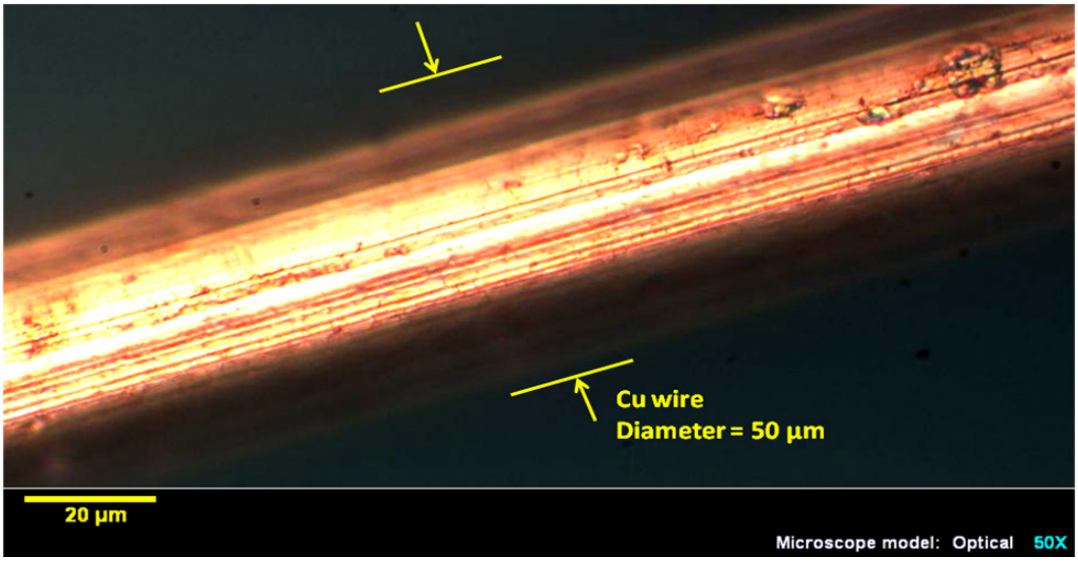

Figure 28. Optical image of unmodified copper wire

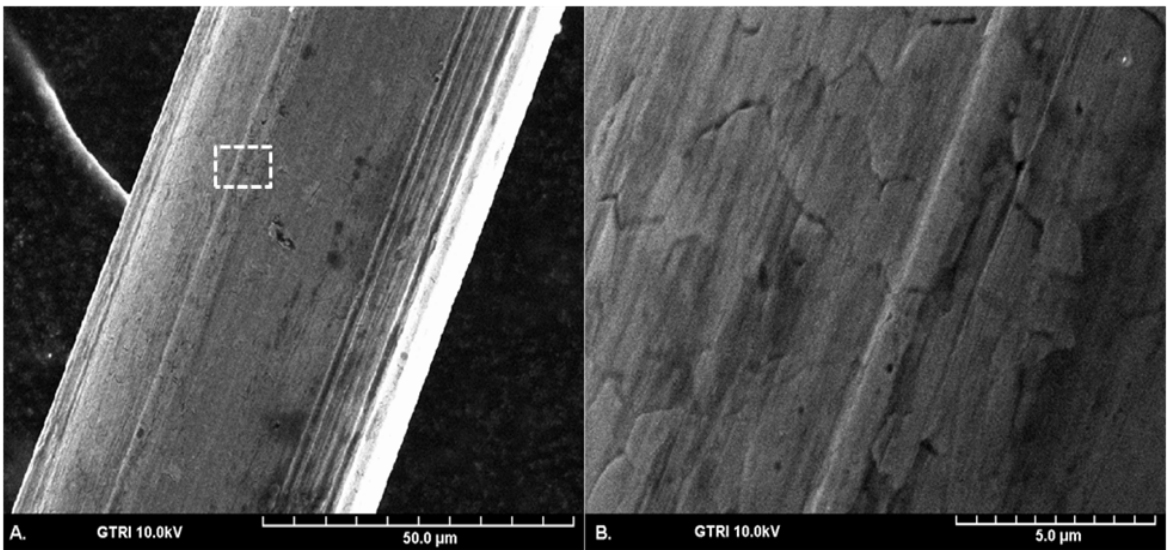

Figure 29. SEM image of uncoated Cu wire: A. Cu wire, B. Close-up wire surface

Figures 30 and 31 are optical and SEM images of the copper wire coated with boron carbide. Microscopy revealed a rough surface resulting from the coating.

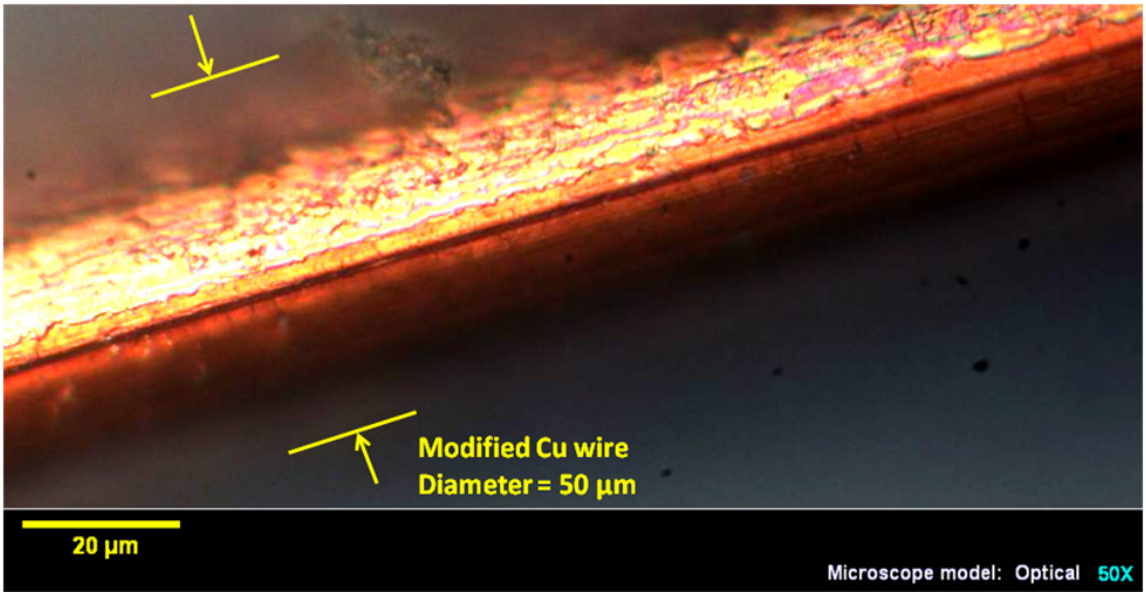

Figure 30. Optical image of coated copper wire

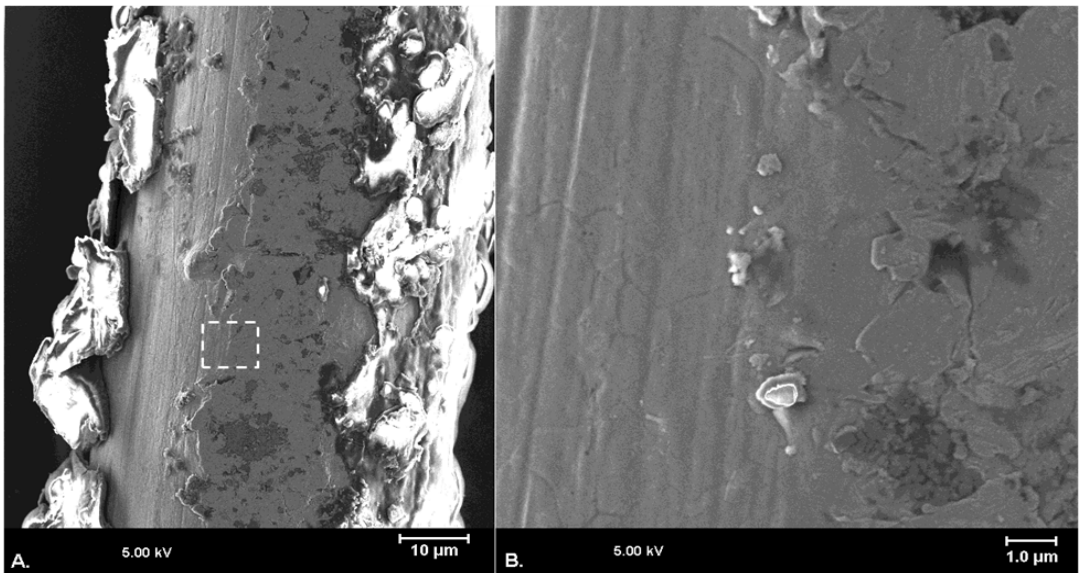

Figure 31. SEM image of coated Cu wire: A. Coated wire, B. Close-up of coating

EDS was also carried out on these samples to confirm the presence of the boron carbide on the surface of the wires. Figure 32 is the EDS spectrum of the coated wire. EDS confirmed the presence of boron on the wire, which is a result from the boron carbide coating, as evident by the boron peak on the spectrum (Figure 32).

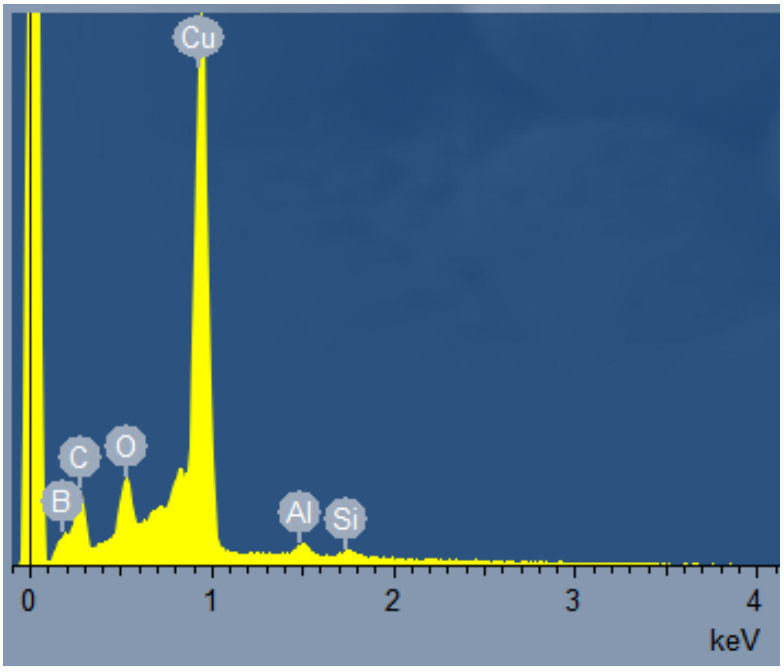

Figure 32. EDS spectrum of copper wire coated with B_4C

As was the case with the Kevlar fibers coated with aluminum and boron carbide, it appears from the images that the coatings on the copper wire are present but are not perfect. The coatings seem to have poor adhesion and show signs of delamination. The lack of good adhesion along with the non-conformal nature of the boron carbide coating may be responsible for the absence of change in the modulus and hardness of the coated Kevlar fibers and copper wires.

CHAPTER 5

CONCLUSIONS

5.1 Nanoindentation on Wires

Nanoindentation tests were conducted on sections of 50 μm copper wire prior to testing on Kevlar. This was done in order to validate the experimental methodology. The results from nanoindentation on the copper wires were commensurate with the tabulated data. Two important conclusions are drawn from these results. First, nanoindentation is a viable method to ascertain the mechanical properties of small diameter wires and fibers. Second, these results validate the sample preparation procedure. This is an important result because it allows for the exploration of the surface properties of wires and fibers using nanoindentation, a task that cannot be achieved using the method described in other studies in which the fiber is encased in epoxy [27, 28].

5.2 Effect of the Boron Carbide Coating

Kevlar fibers were coated with boron carbide and nanoindentation was used to determine the effects of the coating on the mechanical properties of the fibers. Results from nanoindentation did not show any significant changes in the modulus or hardness of the fibers (reduced modulus: 7-17 GPa; hardness: 0.25-1 GPa). SEM and optical microscopy revealed the existence of a coating on the surface of the fibers. EDS confirmed that the coating was indeed boron carbide. This coating, however, did not adhere well and was non-conformal. It is believed that the lack of change in the properties of the fiber may be due to the failure to achieve good adhesion and/or a conformal coating of boron carbide.

Results from the puncture resistance study on boron carbide coated Kevlar and Nomex fabrics indicate that the addition of boron carbide increases the puncture resistance of the fabrics. It was hypothesized that this increase in puncture resistance of the fabric was a result of the enhancement of the mechanical properties of the individual fibers as a result of the nano-scale boron carbide coating. The findings from this nanoindentation study indicate that such improvement in puncture resistance is not due to a change in the hardness or modulus of the modified fiber. Rather, the improvement in puncture resistance is likely due to other mechanisms affected by the boron carbide coating such as increasing the fiber-to-fiber friction and coupling the fibers. These changes in fiber-to-fiber interaction reduce fiber mobility and make it more difficult for penetrating objects to change the fabric structure and push the fibers aside. Increasing the fiber-to-fiber friction and coupling the fibers also helps improve the overall performance of the fabric by transferring the ballistic energy to more fibers [4, 7, 9, 10]. Such improvements of the fabric are likely due to the increase in the surface roughness of the individual fibers as a result of the boron carbide coating. These results are significant because they show that coatings that modify the surface morphology of the fibers are capable of enhancing the overall performance of Kevlar-based soft body armor systems.

5.3 Future Work

Future work in this study includes further investigation into the exact mechanisms by which the addition of a boron carbide coating improves puncture resistance of the coated Kevlar fabric. Additionally, it was shown that coatings on the fibers did not adhere properly and were non-conformal. Further research should be conducted on

different adhesion layer materials such as AlSi [10] and Ti [32] as well as different deposition methods to achieve more uniform coatings with stronger adhesion to the fibers. Once better coatings are achieved, they can be analyzed with nanoindentation to determine their effect on the nano-mechanical properties of the fibers and with puncture and ballistic resistance tests to determine their effect on the macro-mechanical properties of the coated Kevlar fabric. Lastly, these coatings can be optimized to maximize the ballistic resistance of Kevlar-based soft body armor systems without significantly increasing their weight or reducing their flexibility.

APPENDIX A

SCHEMATIC OF SAMPLE PREPARATION AND NANOINDENTATION PROCEDURE

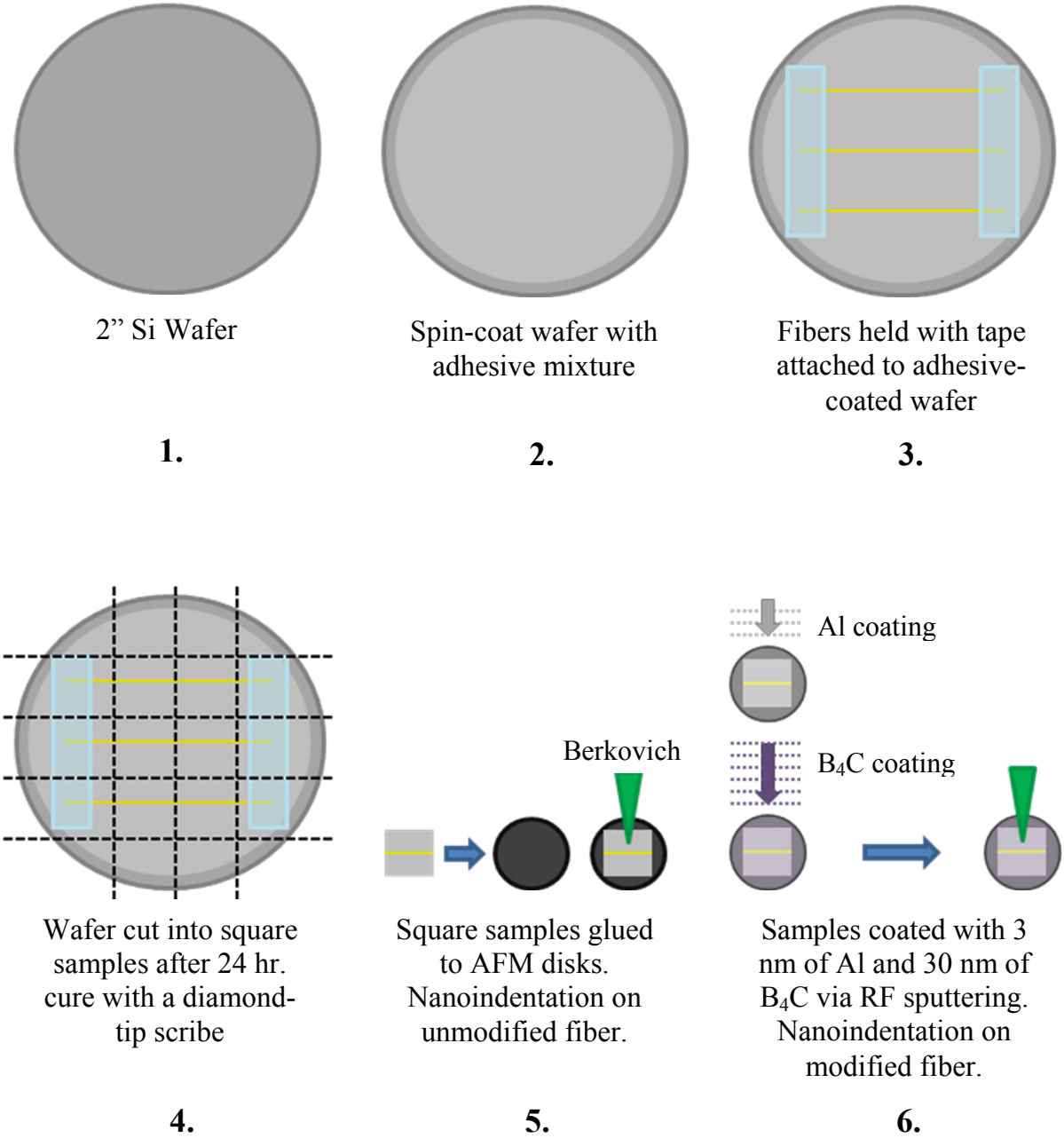

Figure 32. Schematic of sample preparation and nanoindentation procedure

REFERENCES

[1] L. Cannon, "Behind armour blunt trauma--an emerging problem.," *Journal of the Royal Army Medical Corps*, vol. 147, no. 1, pp. 87-96, Feb. 2001.

[2] J. J. Petrovic and K. J. McClellan, "Ceramic/polymer functionally graded material (FGM) lightweight armor system," Los Alamos, 1998.

[3] "Ballistic Resistance of Personal Body Armor," *National Institute of Justice - Law Enforcement and Corrections Standards and Testing Program*, 2001.

[4] Y. S. Lee, E. D. Wetzel, and N. J. Wagner, "The ballistic impact characteristics of Kevlar® woven fabrics impregnated with a colloidal shear thickening fluid," *Journal of materials science*, vol. 38, no. 13, pp. 2825–2833, 2003.

[5] DuPont, "KEVLAR Aramid Fiber: Technical Guide," 2011. [Online]. Available: http://www2.dupont.com/Kevlar/en_US/tech_info/index.html.

[6] B. Cheeseman and T. A. Bogetti, "Ballistic impact into fabric and compliant composite laminates," *Composite Structures*, vol. 61, no. 1–2, pp. 161-173, Jul. 2003.

[7] V. Tan, T. Tay, and W. Teo, "Strengthening fabric armour with silica colloidal suspensions," *International Journal of Solids and Structures*, vol. 42, no. 5–6, pp. 1561-1576, Mar. 2005.

[8] S. Bazhenov, "Dissipation of energy by bulletproof aramid fabric," *Journal of materials science*, vol. 32, no. 15, pp. 4167–4173, 1997.

[9] D. P. Kalman, R. L. Merrill, N. J. Wagner, and E. D. Wetzel, "Effect of particle hardness on the penetration behavior of fabrics intercalated with dry particles and concentrated particle-fluid suspensions.," *ACS applied materials & interfaces*, vol. 1, no. 11, pp. 2602-12, Nov. 2009.

[10] R. Gadow and K. V. Niessen, "Lightweight ballistic structures made of ceramic and cermet/aramide composites," *Ceramic Transactions*, pp. 3–18, 2003.

[11] H. A. Barnes, "Shear-Thickening ('Dilatancy') in Suspensions of Nonaggregating Solid Particles Dispersed in Newtonian Liquids," *Journal of Rheology*, vol. 33, no. 2, p. 329, 1999.

[12] S. Ulrich, H. Ehrhardt, J. Schwan, R. Samlenski, and R. Brenn, "Subplantation effect in magnetron sputtered superhard boron carbide thin films," *Diamond and Related Materials*, vol. 7, no. 6, pp. 835-838, Jun. 1998.

[13] H. Chen, J. Wang, H. Yang, W. Z. Li, and H. Li, "Synthesis of boron carbide films by ion beam sputtering," *Surface and Coatings Technology*, vol. 128–129, no. 1, pp. 329-333, Jun. 2000.

[14] F. Thévenot, "Boron carbide—A comprehensive review," *Journal of the European Ceramic Society*, vol. 6, no. 4, pp. 205-225, Jan. 1990.

[15] T. Hu et al., "Structures and properties of disordered boron carbide coatings generated by magnetron sputtering," *Thin Solid Films*, vol. 332, no. 1–2, pp. 80–86, 1998.

[16] J. Sun et al., "Chemical structure and micro-mechanical properties of ultra-thin films of boron carbide prepared by pulsed-laser deposition," *Tribology Letters*, vol. 17, no. 1, pp. 99–104, 2004.

[17] Z. Han, G. Li, J. Tian, and M. Gu, "Microstructure and mechanical properties of boron carbide thin films," *Materials Letters*, vol. 57, no. 4, pp. 899–903, 2002.

[18] T. Tavsanoglu, S. Labdi, and M. Jeandin, "Synthesis and Characterization of Boron Carbide Thin Films Grown by Rf Sputtering," *TMS 2009 138th Annual Meeting & Exhibition; supplemental proceedings*, vol. 1, pp. 573-580, 2009.

[19] M. Cheng, W. Chen, and T. Weerasooriya, "Mechanical Properties of Kevlar® KM2 Single Fiber," *Journal of Engineering Materials and Technology*, vol. 127, no. 2, p. 197, 2005.

[20] Hysitron, "Hysitron Nanomechanical Testing Probe Selection," 2010. [Online]. Available: http://www.hysitron.com/products/ti-series.

[21] W. C. Oliver and G. M. Pharr, "An improved technique for determining hardness and elastic modulus using load and displacement sensing indentation experiments," *Journal of Materials Research*, vol. 7, no. 06, pp. 1564-1583, Jan. 1992.

[22] M. F. Doerner and W. D. Nix, "A method for interpreting the data from depth-sensing indentation instruments," *Journal of Materials Research*, vol. 1, no. 04, pp. 601-609, Jan. 1986.

[23] S. I. Bulychev, V. P. Alekhin, M. H. Shorshorov, A. P. Ternovskii, and G. D. Shnyrev, "Determining Young's Modulus From the Indentor Penetration Diagram," *Zavodskaya Laboratoriya*, vol. 41, no. 9, pp. 1409-1412, 1975.

[24] N. A. Stilwell and D. Tabor, "Elastic Recovery of Conical Indentations," *Proceedings of the Physical Society*, vol. 78, no. 2, pp. 169-179, Aug. 1961.

[25] I. Sneddon, “The relation between load and penetration in the axisymmetric boussinesq problem for a punch of arbitrary profile,” *International Journal of Engineering Science*, vol. 3, no. 1, pp. 47-57, May 1965.

[26] G. Pharr, “Measurement of mechanical properties by ultra-low load indentation,” *Materials Science and Engineering A*, vol. 253, no. 1–2, pp. 151-159, Sep. 1998.

[27] J. a. Bencomo-Cisneros et al., “Characterization of Kevlar-29 fibers by tensile tests and nanoindentation,” *Journal of Alloys and Compounds*, pp. 29-32, Nov. 2011.

[28] J. Graham, C. McCague, O. Warren, and P. Norton, “Spatially resolved nanomechanical properties of Kevlar fibers,” *Polymer*, vol. 41, no. 12, pp. 4761–4764, 2000.

[29] T. H. Courtney, *Mechanical Behavior of Materials*. New York: McGrill-Hill, 1990, pp. 80-136, 263-324.

[30] S.-Y. Chang and T.-K. Chang, “Grain size effect on nanomechanical properties and deformation behavior of copper under nanoindentation test,” *Journal of Applied Physics*, vol. 101, no. 3, p. 033507, 2007.

[31] Y. Y. Lim and M. M. Chaudhri, “The influence of grain size on the indentation hardness of high-purity copper and aluminium,” *Philosophical Magazine A*, vol. 82, no. 10, pp. 2071-2080, Jul. 2002.

[32] T. Eckardt, K. Bewilogua, and G. V. D. Kolk, “Improving tribological properties of sputtered boron carbide coatings by process modifications,” *Surface and Coatings*, pp. 69-75, 2000.